Model Calculations of the Ionosphere of Titan during Eclipse Conditions

Karin Ågren

Luleå University of Technology

Swedish Institute of Space Physics, Uppsala

April 24, 2006

Abstract

This report is based on data from the Cassini spacecraft and the main aim of this work is to model the ionosphere of Titan and compare it with data from the sixth flyby (T5). It occurred April 16, 2005, and was chosen as it was a nightside pass of the moon. We have shown that magnetospheric impacting electrons alone can account for the observed ionisation during T5.

Data from Cassini show that the main constituents of Titan's atmosphere are molecular nitrogen, methane and molecular hydrogen, with nitrogen being the most common species at low altitudes. There are also several minor species contributing to the chemical reactions taking place in the atmosphere. Of these HCN, HC_3N and C_2H_4 are of certain relevance for this work.

A method by M. H. Rees is used to calculate the ionisation rate height profiles. It can be shown that modifications of the flux value change the magnitude of the ionisation rate and that the electrons penetrate deeper into the ionosphere the more energy they are given.

For electrons of energies lower than 200 eV the ionisation rate cannot be calculated by the method mentioned above. We therefore have to introduce a model by Prof. D. Lummerzheim to infer the ionisation rates of lower energy electrons in order to achieve a more complete picture. Combining the results, we can look at the dependence between the ionisation maxima in kilometres and the electron energy. The electrons penetrate deeper into the ionosphere given more energy, with a steep gradient for low energies, which gradually decreases for higher energies.

By looking at the main chemical reactions that take place in Titan's ionosphere we can calculate the densities of the ion species. These results are compared with actual data with good agreement. Finally, we look at the electron density received from our model and compare it to the density measured by the Langmuir probe on Cassini, which leads us to the conclusion that magnetospheric electrons do account for the observed electron density.

Sammanfattning

Det här arbetet är baserat på data från rymdfarkosten Cassini och går ut på att modellera Titans jonosfär för de omständigheter som rådde vid den sjätte förbiflygningen. Den skedde den 16 april 2005 och valdes eftersom Cassini vid det tillfället passerade Titan på skuggsidan. Vi visar att magnetosfärselektroner står för den observerade jonisationen av atmosfären vid denna passage.

Data från Cassini visar att Titans atmosfär huvudsakligen består av kväve, men att även metan och väte finns i relativt stora mängder. Förutom dessa finns det också många mindre vanliga ämnen som bidrar till de kemiska reaktionerna i Titans jonosfär. Av dessa är HCN, HC_3N och C_2H_4 av särskild vikt för detta arbete.

En given metod används för att beräkna jonisationsgraden vid olika höjder. Jonisationsgraden är beroende av elektronflödet, elektronenergin, energiförlustfunktionen, massdensiteten och energiförlusten per jon som formas. Elektronflödet och elektronenergin varieras för att se hur jonisationsprofilerna förändras av detta. Det visar sig att ändringar i flödet leder till en direkt ändring av jonisationsgraden, medan en ökning av energin leder till att elektronerna tränger djupare ner i jonosfären.

För elektroner med energi under 200 eV kan ovan nämnda metod inte appliceras. Vi inför därför en alternativ modell för att kunna bestämma jonisationsgraden för elektroner av låga energier och på så sätt få en komplett bild av jonisationen. Genom att kombinera resultaten kan vi studera beroendet mellan jonisationsmaximat i kilometer och elektronenergin. Ju energirikare elektronerna är, desto djupare tränger de ner i jonosfären.

Genom att studera huvudreaktionerna i Titans jonosfär kan vi modellera densiteterna av de viktigaste jonerna. Detta resultat jämförs med faktisk data från Titan och visar god överensstämmelse. Vi använder oss slutligen av den modellerade elektrondensiteten och jämför den med densiteten som uppmätts av Langmuirsonden, vilket bekräftar att magnetosfärselektroner svarar för den observerade jonisationen.

CONTENTS

CHAPTER 1

INTRODUCTION

Titan was for the first time observed by the Dutch scientist Christiaan Huygens in 1655. While studying Saturn and its rings, he discovered the presence of a moon in orbit, and ever since Titan has fascinated scientists all around the world. For more than 300 years, 325 to be exact, researchers were left to make ground-based observations of the mysterious moon, but in 1980 the first eagerly awaited encounter with Titan took place.

The first flybys of Titan were made by the Voyager probes in late 1980 and 1981.[1] The Voyager spacecraft were not sophisticated enough to make any detailed exploration of the satellite, especially not as Titan's surface was hidden by a dense, photochemical haze. Voyager 1, however, managed to determine Titan's surface diameter to 5150 km by radio occultation. That makes Titan the second largest moon in our solar system, rivalled only by Ganymede, Jupiter's largest moon. The Hubble Space Telescope succeeded the Voyager spacecraft in the exploration of Titan. Hubble did observations in the infrared and discovered the existence of dark and light regions on Titan, now known as Xanadu and the Sickle.

In the summer of 2004, the Cassini spacecraft arrived at Saturn after a seven year long journey through interplanetary space. Cassini is by far the most interdisciplinary spacecraft ever flown and has – and will for many years to come – provided scientists with interesting data to analyse. The spacecraft will not only make close studies of Saturn and its rings, but also conduct flyby studies of Saturn's moons and collect data that will increase our understanding of their composition, structure and interaction with the space environment. To date, 34 moons of Saturn have been officially named, with new moons still being found. Among these numerous moons Titan is considered to be the most interesting one, as it is one of the few natural satellites in the solar system that have their own

---

[1]Voyager 1 and Voyager 2.

thick atmosphere.

This report is based on data from the Cassini spacecraft. The main purpose is to do a model of the ionosphere of Titan which later can be used to try finding a spectrum of the incoming electrons. This will be preceded by looking at the neutral atmosphere of Titan. The neutral atmosphere is needed to calculate ionisation rates at different heights. Knowing these rates one may compute the densities of different ion species and therefrom deduce the electron density. The last step is to look at electron densities from Cassini, measured in the ionosphere of Titan, and try to find the electron spectrum needed to provide the measured profile.

Chapter 2

Titan

From a terrestrial view Titan may be the most interesting object in the solar system. What makes it so special is the fact that Titan possesses a thick atmosphere, even denser than the one on Earth. Figure 2.1 shows approximately what Titan would look like to the human eye. The images to create the composite are taken with the Cassini spacecraft wide angle camera during the sixth flyby of Titan on April 16, 2005. The orange colour is due to mostly hydrocarbon and polycyanide particles which make up Titan's atmospheric haze. There are reasons to believe that the processes taking place in the atmosphere of Titan are similar to those that took place on the primordial Earth some 4 billion years ago. Studying the atmosphere of Titan could possibly give clues to our understanding of the origin of life on Earth.

Titan has a diameter of 5150 km – larger than both Mercury and Pluto – and a mean density of approximately 1.88 $g^{-1}cm^3$. That is about twice the density of ice, which implies that Titan is made up of mostly ice with some small amount of rock in the centre. The atmospheric pressure on Titan is considerably higher than on Earth. The pressure on Earth is known to be 1 bar, whereas the Titan pressure is 60% higher; 1.6 bars.

2.1 Titan's ionosphere

The composition of Titan's atmosphere near the surface is over 97% molecular nitrogen. The remaining three percent are made up by methane and other minor species. The atmosphere is highly ionised, which gives rise to an ionosphere. This ionosphere is highly variable, as it is dependent on where Titan is situated in relation to Saturn. Titan orbits Saturn at a distance of 20.3 R_S [1]. Saturn is
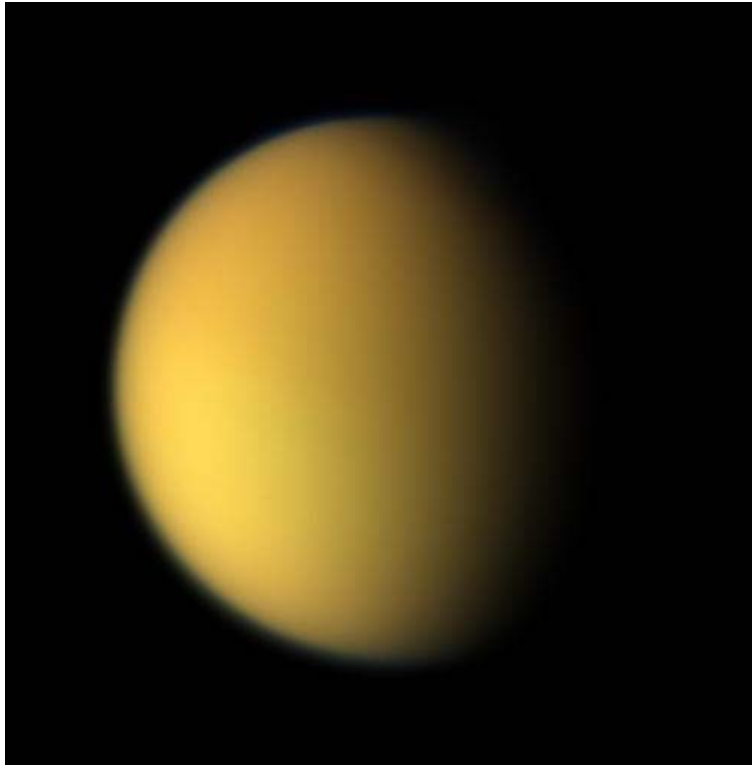
Figure 2.1: Cassini's view of Titan. Image from NASA/JPL/Space Science Institute.

surrounded by a huge magnetosphere that is corotating with the planet.[1] With respect to the Saturnian magnetosphere there are principally three conditions that may apply to the moon, since a certain point on Titan may either be sunlit, dark or in between. Figure 2.2 shows how different conditions may arise.

Titan's lack of a measurable intrinsic magnetic field indicates that it has no electrically conducting and convecting liquid core. The moon's interaction with Saturn creates an induced magnetic wake behind Titan. The magnetospheric plasma velocity around Titan is subsonic and superalfvenic, which leads to that no bow shock forms in front of Titan [1]. As the plasma enters Titan's exosphere it is gradually slowed by mass-loading of the heavy and slower ionospheric ions into the faster and thinner magnetospheric plasma. At the same time, the magnetic field strength increases. The magnetic field piles up until it eventually drapes around the moon. This is expected to be the dominant source of pressure against the ionosphere [2].
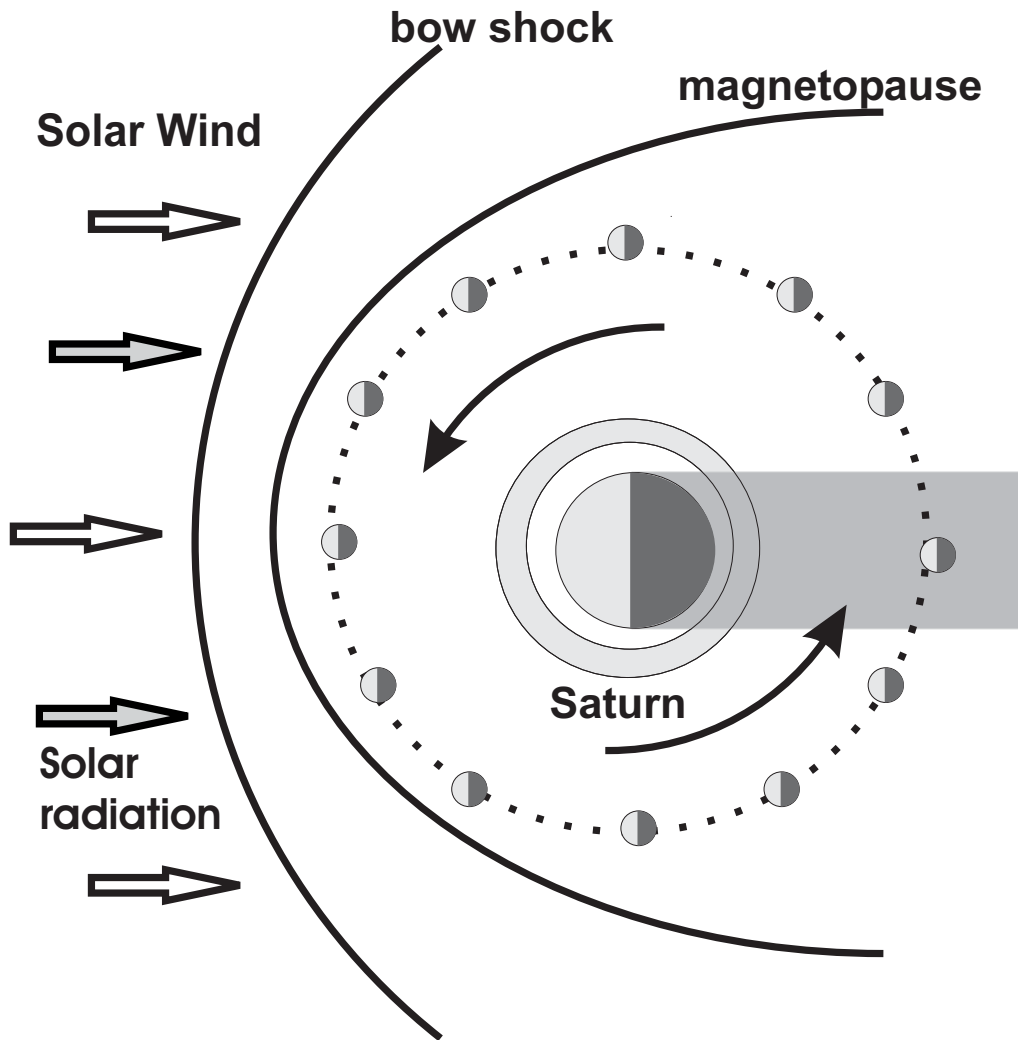
---

[1]At least outside 6 R_S.

Figure 2.2: Titan's orbital phase. Courtesy of R. Modolo.

There are four different sources that are considered to be responsible for the ionisation of Titan's atmosphere: solar extreme ultraviolet (EUV) radiation and photoelectrons produced by EUV radiation, magnetospheric electrons and associated secondary electrons created in the impact ionisation process, cosmic rays and proton (and other ion) precipitation. Among these, EUV and magnetospheric electron impact ionisation are the dominant ones [1]. The variation of these sources depends on the location of Titan in Saturn's magnetosphere. This report is based on data from the sixth flyby of Titan. It was made during an eclipse and therefore only the magnetospheric electrons were considered [1].

CHAPTER 3

CASSINI-HUYGENS

Cassini-Huygens is an international collaboration between NASA, ESA, the Italian Space Agency and numerous instrument suppliers from institutions in Europe and the US. The Cassini orbiter was provided by NASA's Jet Propulsion Laboratory, the Huygens probe was built by ESA and the Italian Space Agency provided Cassini's high-gain communication antenna. The Cassini-Huygens mission is by far the most deliberate attempt to explore Titan and its complex atmosphere. The mission consists of an orbiter, Cassini, and a landing probe, Huygens. The launch of the spacecraft took place in October 1997 and slightly less than seven years later, in July 2004, it reached Saturn. The mission so far has proved to be very successful and both the probe and the spacecraft have provided scientists with a considerable amount of interesting data.

3.1   Instruments onboard Cassini

Cassini is equipped with a total of twelve science instrument packages. Each instrument package is designed to carry out various scientific studies of Saturn and its moons. We will now provide a brief introduction to the ones that have contributed to the work presented in this thesis.

3.1.1   Radio and Plasma Wave Science

The main task of the Radio and Plasma Wave Science (RPWS) package is receiving and measuring the radio signals coming from Saturn, including the radio waves given off by the interaction of the solar wind with Saturn and Titan. The major components of the instrument package are three electric field sensors, a magnetic search coil assembly and a Langmuir probe. For this report, the electron density near Titan determined by the Langmuir probe is of greatest relevance.
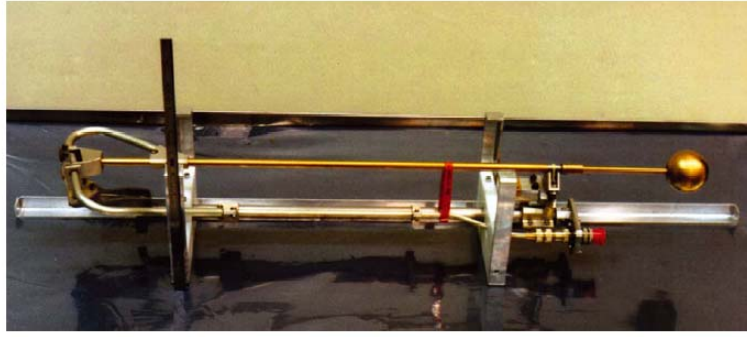
Figure 3.1: The Langmuir probe onboard Cassini [3].

Langmuir probe

The Langmuir probe can determine a range of parameters including plasma density and plasma temperature. The name 'Langmuir probe' arises from the fact that the basic theory was founded by Langmuir in the 1920s. The Langmuir probe onboard Cassini is a titanium sphere, about 50 mm in diameter, placed on a 1.5 m boom. Inserted into a plasma, this sphere will attract charged particles. If the probe is negatively charged, this current consists of probe photo electrons and all the ions, but only the electrons that have a velocity above a certain velocity towards the probe. This threshold velocity is dependent on the potential of the conductor (sensor). A positively charged probe attracts a current consisting mainly of electrons. For a spherical probe with a positive bias, the electron current, I_e, and the ion current, I_i, in a stationary plasma can be written in its simplest form, according to the OML-theory,[1] as

$$I_e = I_{e0}(1 - \chi_e) \tag{3.1}$$

and

$$I_i = I_{i0}e^{-\chi_i}, \tag{3.2}$$

where

$$\chi_j = \frac{q_j(U_B + U_{sc})}{k_B T_j} \tag{3.3}$$

and

---

[1]Orbital Motion Limited.

$$I_{j0} = -A_{\mathrm{P}} n_j q_j \sqrt{\frac{k_{\mathrm{B}} T_j}{2\pi m_j}}. \tag{3.4}$$

In the above equations q_j is the charge of the particle species j, U_{B} is the bias voltage to the probe, U_{sc} is the spacecraft potential, $k_{\mathrm{B}} = 1.380658 \times 10^{-23}$ J K^{-1} is the Boltzmann constant, T_j is the temperature of the particle species, A_{P} is the area of the sphere and n_j is the number density of the particle species. The minus sign indicates that the flow from the probe to the plasma is set to be positive. From Equation 3.4 follows that with a given probe current, the density and the temperature can be estimated. The total current is given by the sum of the electron and the ion current and depends on the bias potential. This relation can be displayed as a typical U–I curve, which is shown in Figure 3.2. As can be seen, for high positive or negative values of the bias voltage the relationship is linear. The U–I characteristics is one of the most important tools when using Langmuir probes [4]. This was a brief introduction to the Langmuir probe onboard Cassini. A full treatment requires a more rigorous theory, see [3].
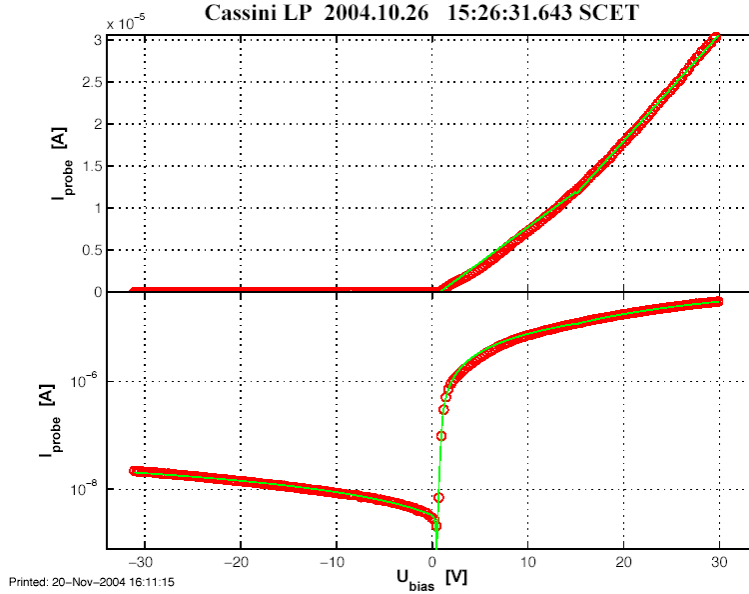

Figure 3.2: A sweep made by the Langmuir probe from the first flyby, TA. Courtesy of J.-E. Wahlund.

3.1.2 Ion and Neutral Mass Spectrometer

The Ion and Neutral Mass Spectrometer (INMS) determines the composition and structure of positive ions and neutral particles in the upper atmosphere of Titan. The instrument can determine the chemical, elemental and isotopic composition of the gaseous and volatile components of the neutral particles and the low energy ions in Titan's atmosphere and ionosphere. Two of the scientific objectives of INMS are to study Titan's atmospheric chemistry and to investigate the interaction of Titan's upper atmosphere with the magnetosphere and solar wind.

3.1.3 Cassini Plasma Spectrometer

The Cassini Plasma Spectrometer (CAPS) explores plasma within and near Saturn's magnetosphere. This is done by measuring the energy and the electric charge of the particles, i.e. electrons and protons, that the instrument encounters. The instrument is used to study the composition, density, flow, velocity and temperature of the ions and electrons. CAPS consists of three different sensors: an ion mass spectrometer, an ion beam spectrometer and an electron spectrometer. The electron spectrometer measures the energy of the incoming electrons and has an energy range between 0.7 and 30000 eV.

3.2 Huygens

The Huygens probe was made to descend through Titan's atmosphere and land on the moon. During the seven year-long journey to Saturn Huygens rode piggyback on Cassini. The lander was set free on the 25th of December 2004 and 20 days later, the 14th of January 2005, it touched down on Titan. Huygens was the first spacecraft to land on a moon in the outer solar system. The lander was equipped with six science instrument packages designed to study the content and dynamics of Titan's atmosphere and collect data and images on the surface. These data was sent to Cassini, which amplified the signals and sent them back to Earth.

3.3 Cassini Titan flybys

There are 44 planned flybys of Titan,[2] of which eleven have taken place at the time of writing. Each flyby has its own unique conditions. The flyby may occur

---

[2]Not including a possible extension of the mission.

on the sunlit side or in the shadow, through the wake or in front of the planet, at noon or in the middle of the night. The environment is also strongly influenced by the altitude of the flyby and the region where Titan is located at the time (magnetosphere, magnetosheath, solarwind). Evaluating these different flybys and comparing them to each other gives a better and more complete picture of Titan than just a single flyby could do.

3.3.1 The sixth flyby of Titan – T5

This thesis is based on the conditions that apply to the sixth flyby of Titan, i.e. T5.[3] T5 took place on the 16th of April 2005 and the closest approach occurred at a distance of 1025 km above the moon's surface. Figure 3.3 shows the path of the sixth flyby. It is also given where the Sun, Saturn and Titan's wake was located at the time of the flyby. There are several reasons why T5 was chosen for conducting this study.

- INMS, CAPS and RPWS data was collected during the flyby. As the report is based on these data, this was a requirement. The INMS does not sample ion data at each flyby. INMS requires a certain spacecraft attitude towards the ram flux direction to be able to collect data.

- The flyby is rather deep in comparison to the others. Having a closest approach of only 1025 km gives a more complete picture of the entire ionisation altitude profile.

- The data was collected during a nightside pass, which means that the photoionisation was not an important ionisation source. We therefore assume that magnetospheric impacting electrons alone can account for the observed ionisation.

---

[3]The flybys are called TA, TB, TC, T3, T4 and T5 etc.
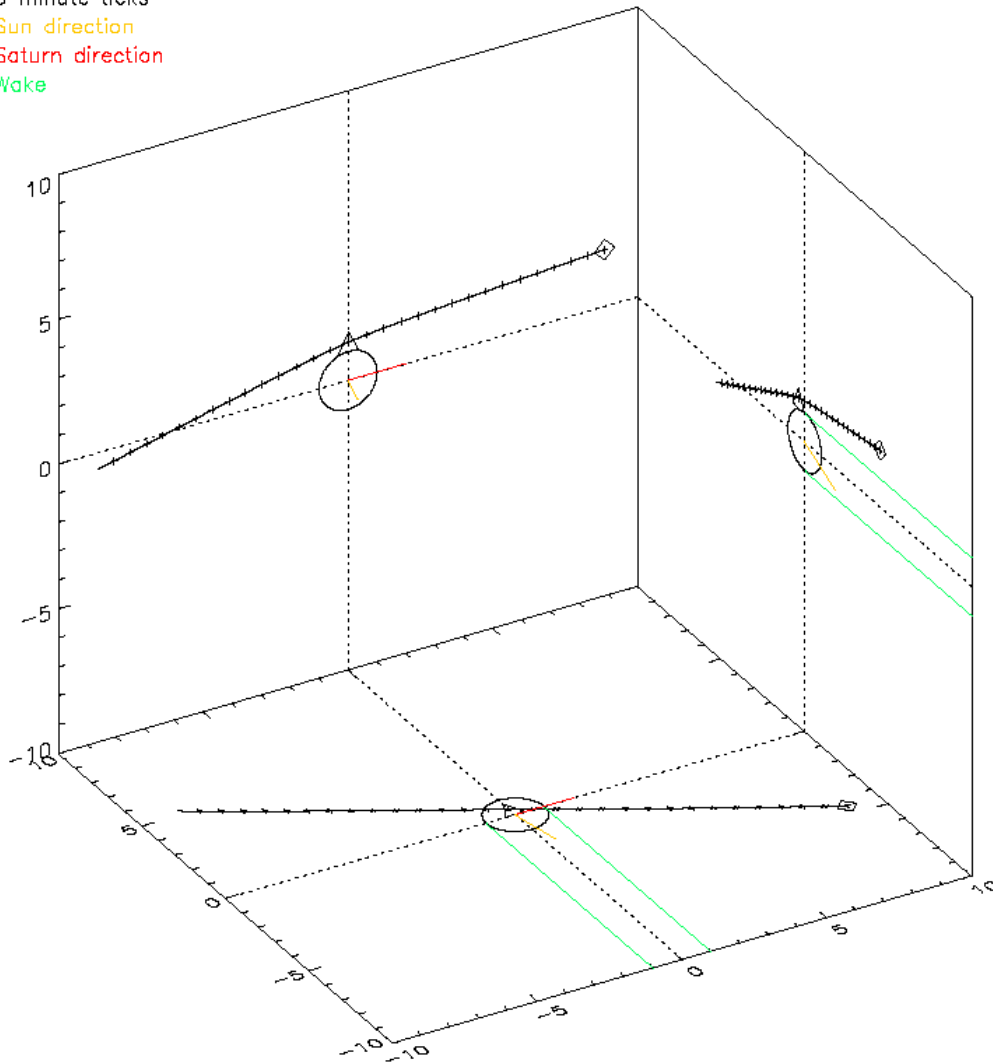
Figure 3.3: The sixth flyby of Titan, April 16, 2005. Figure from F. Crary, CAPS team.

CHAPTER 4

THE NEUTRAL ATMOSPHERE

4.1   Major neutral constituents

The main constituent of Titan's atmosphere is molecular nitrogen (97% near the surface). The rest is principally made up by methane and molecular hydrogen. Vertical profiles of the main atmospheric constituents could be received from data collected by the Ion and Neutral Mass Spectrometer, INMS, during T5.[1] These values were considered by R. Yelle, who came up with an empirical model for the upper atmosphere of Titan [5].

As shown in Figure 4.1, nitrogen is the major neutral species between 1000 and 1800 km, with hydrogen taking over at higher altitudes. The fact that the hydrogen line almost adapts to a constant value of density at approximately 1500 km gives a signature of upward flux. In other words; a lot of hydrogen seems to be escaping from the moon. Using Yelle's atmospheric profiles [5], we tried to find suitable equations to fit the two main constituents, i.e. nitrogen and methane, to the data. The equations we derived are respectively:

$$\rho_{N_2} = e^{137} x^{-16.5}, \tag{4.1}$$

$$\rho_{CH_4} = e^{89.7} x^{-10.3}, \tag{4.2}$$

where x is the altitude given in kilometres. Plotting these equations in the same interval as the model [5] gives rise to Figure 4.2.

The forthcoming modelling is based on this neutral atmosphere, with nitrogen being the most important constituent at lower altitudes. As seen in Figure 4.2, at an altitude of 1000 km nitrogen is more common than methane by a factor of approximately 70.
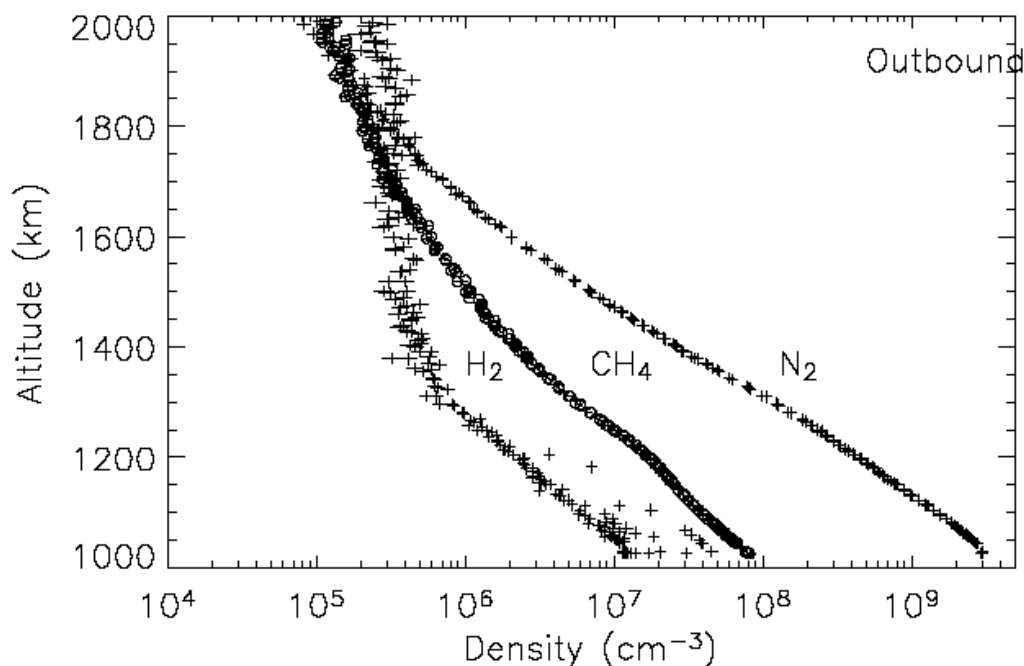
---

[1]Outbound trajectory.

Figure 4.1: INMS neutral atmosphere. From [5].

4.2   Minor neutral constituents

Nitrogen and methane being the major species on Titan, there are several minor species that also contribute to the chemical processes taking place in the iono-sphere. Photochemistry plays a key role in the structure of Titan's atmosphere [6]. After the Voyager encounter with the Saturnian moon, Y. L. Yung made a detailed model of the photochemistry of Titan's atmosphere. This was published in 1984 by Yung et al., with an update by Yung in 1987 [7, 8]. A little less than ten years later, D. Toublanc et al. developed a new photochemical model of the moon's atmosphere, which included all the important compounds and reactions in spherical geometry from the surface to 1240 km [6].

The profile of HCN was received from Dr. Ingo Müller–Wodarg at Imperial College in London. The profile is not based on measurements, but 'tuned' to give the right temperatures. These temperatures are derived from the N_2 and CH_4 densities observed by Cassini. The model is based on the fact that HCN is the main gas regulating Titan's temperatures. The more HCN there is, the cooler the atmosphere gets. This follows from HCN being a very effective emitter of infrared light. Thus, by knowing the solar heating and the expected temperature it is possible to computationally derive what HCN should be. However, the
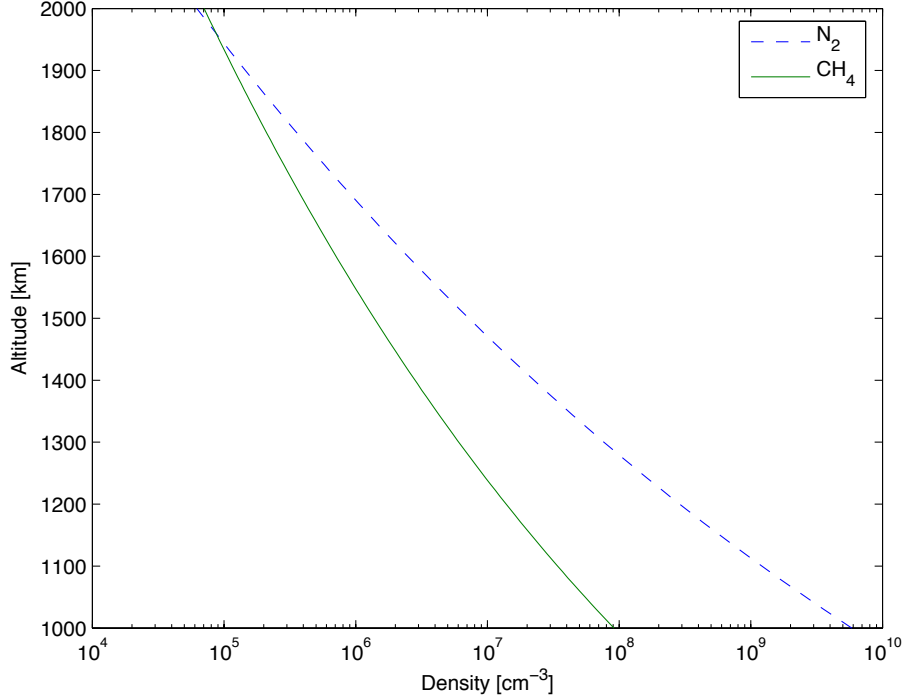
Figure 4.2: Neutral atmosphere.

calculation is complicated as one also has to include the radiative transfer, i.e. IR emitted from HCN hitting other molecules and heating them instead of simply escaping to space [9, 10]. The exact values of the profile can be seen in Appendix A. The highest altitude given is 1667 km. For altitudes above this the Toublanc model was used, as the two models coincide at that altitude.

In this work we develop an ionospheric model using the various neutral atmospheric models. The major constituents, N_2 and CH_4, are taken from the Yelle model based on INMS data, as described in Section 4.1. The minor constituents that are of certain importance for this thesis, HC_3N, C_2H_4 and HCN, are derived from work done by Toublanc [6], Yung [7, 8] and Müller–Wodarg [10]. In Figures 4.3 and 4.4 the density profiles for these three species are shown.
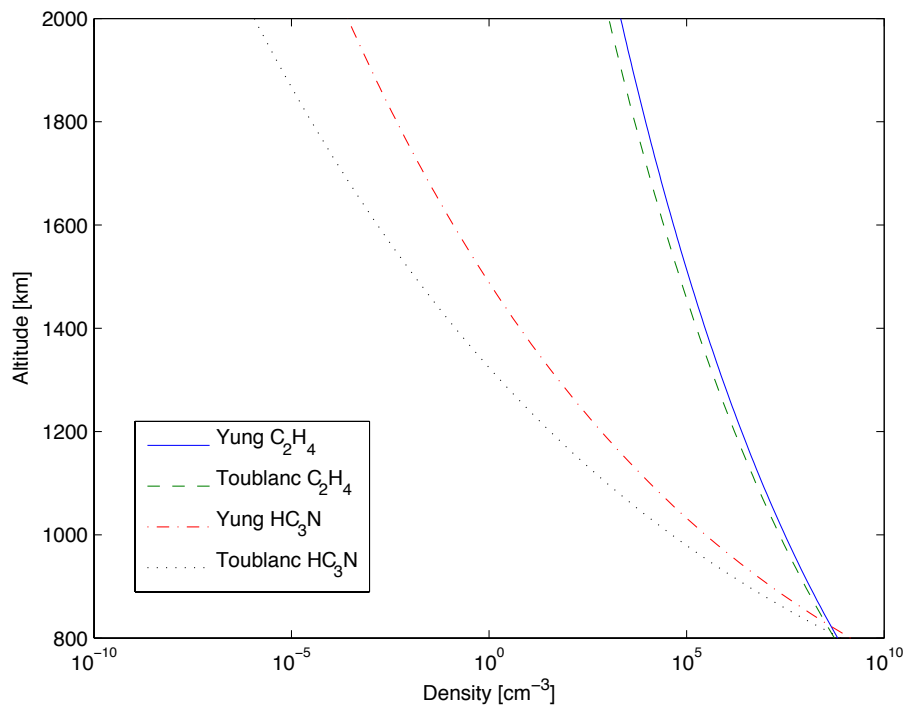
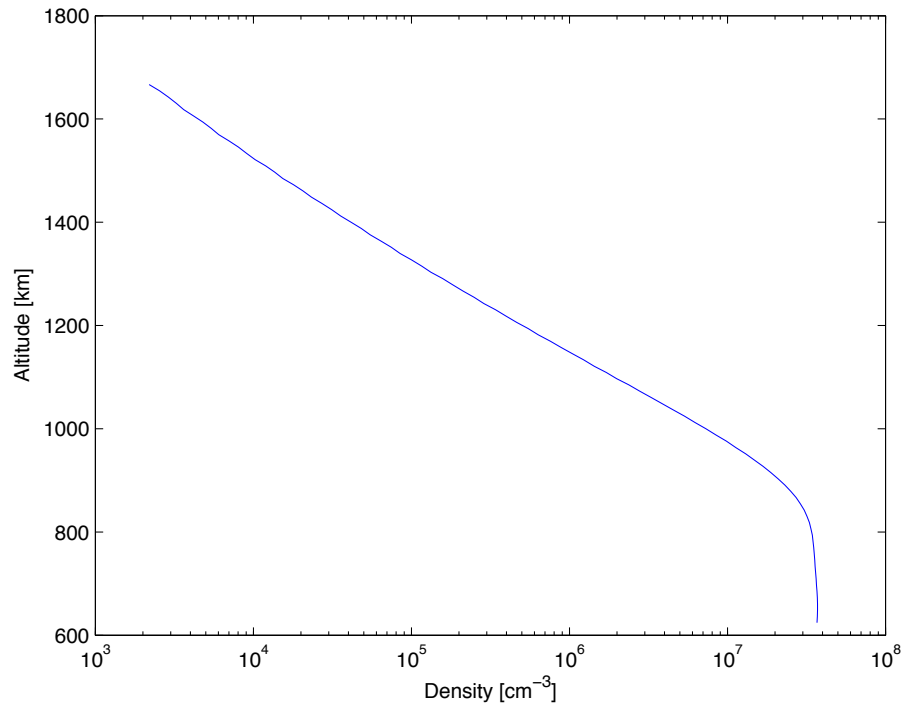Figure 4.3: Density profiles of N_2 and CH_4 in Titan's atmosphere. Based on the models [6, 7, 8].

Figure 4.4: Density profile of HCN in Titan's atmosphere. From [10].

CHAPTER 5

IONISATION CALCULATIONS

5.1 Ionisation rate

A method developed by M. H. Rees [11] permits computation of ionisation rate height profiles in a given model atmosphere. In this model, the energy deposition for monoenergetic electrons at energy E, $\varepsilon(z, E)$, can be expressed by

$$\varepsilon(z, E) = q(z) \triangle \varepsilon_{\text{ion}}, \tag{5.1}$$

where $q(z)$ is the ionisation rate [cm^{-3}s^{-1}] and $\triangle\varepsilon_{\text{ion}}$ the energy loss per ion formation [eV]. As Titan's upper atmosphere mainly consists of N_2 we use the experimentally found value for this species, 37 eV [11]. Further, $\varepsilon(z, E)$ can be expressed as

$$\varepsilon(z, E) = \frac{FE\lambda\left(\frac{s}{R}\right)\rho(z)}{R(E)}. \tag{5.2}$$

Combining 5.1 and 5.2, we get the equation for the ionisation rate:

$$q(z) = \frac{FE\lambda\left(\frac{s}{R}\right)\rho(z)}{R(E) \triangle \varepsilon_{\text{ion}}}, \tag{5.3}$$

where F is the electron flux [cm^{-2} s^{-1}], E is the energy of the incoming electrons [eV], $\lambda\left(\frac{s}{R}\right)$ is the energy dissipation function, which will be discussed in more detail in Section 5.2, $\rho(z) = n_n(z)m_n(z)$ is the density dependent on the height [g cm^{-3}], also known as mass density, s is the atmospheric scattering depth [g cm^{-2}] given by

$$s = \int_z^\infty \rho(z')dz' \tag{5.4}$$

and $R(E)$ is the effective range [g cm^{-2}] given by

$$R(E) = 4.30 \times 10^{-7} + 5.36 \times 10^{-6} E^{1.67} \qquad (5.5)$$

where E is in keV. The effective range is the maximal penetration depth for an electron of a certain energy. The above Equation (5.5), however, is only valid for an energy interval of 200 eV $< E <$ 50 keV. That is due to the fact that the effective range is dependent on the assumption that the average energy loss in an ionising collision is constant. This breaks down for low energy incident electrons, as excitation collisions that do not ionise become more and more important, and thus the average energy loss per ionisation is getting larger and larger. How to achieve the ionisation rates for electrons of lower energies is explained in Chapter 5.5, on page 23.

5.2 Energy dissipation

It can be shown that most of the ionisation and excitation in normal aurorae on Earth is produced by energetic electrons. In the fifties, A.E. Grün and L.V. Spencer chose two different approaches to try explaining how that works. They considered three angular distributions for the incident electron stream; a unidirectional beam, a distribution varying as the cosine of the pitch angle and an isotropic distribution. A number of height profiles could be computed using various energy distribution functions for the primary electrons. Spencer made theoretical computations of the energy dissipation of fast mono-energetic electrons with initial energy, ϵ_0. These electrons were simulated to pass through various absorbing materials, including air. Grün considered the same problem but, unlike Spencer, he made an experimental approach. Using air as the absorber the energy dissipation or absorption was derived from the luminosity produced in the gas. Since the energy loss per ion formed is nearly constant over at wide range of energy this could be used to define the ionisation rate. Spencer's and Grün's results for $\epsilon_0 = 32$ keV showed perfect agreement except near the end of the electron's range. Integrating numerically over an assumed angular distribution provides a method for computing the energy dissipation distribution function for any arbitrary pitch angle distribution of primary auroral electrons [12].

Figure 5.1 shows normalised energy dissipation distributions for four different cases: a monodirectional beam, an incident electron stream varying as the cosine of the pitch angle and for beams with an isotropic angular distribution for pitch angles between 0°and 80°and between 0°and 70°.

In this report two of the angular distributions for the incoming electron stream are
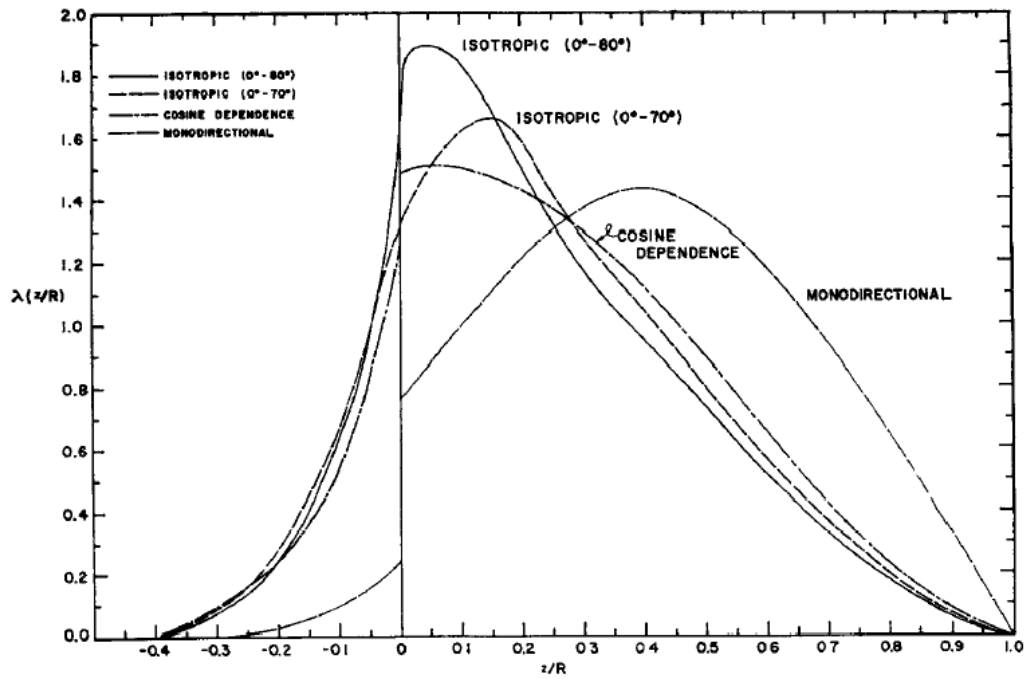
Figure 5.1: Energy dissipation distribution function for four angular dispersions of the incident electron stream [12].

considered: the unidirectional beam and the isotropic distribution between 0°and 80°. The unidirectional stream is chosen as the cold electrons enters the Titan ionosphere at extremely high speeds. One may consider them to be equivalent to a flux of particles of a certain energy from a particular direction; in other words a unidirectional stream. On the other hand, one may also consider the electrons as a thermal population; a hot gas of electrons that enters the ionosphere from many directions at the same time. This would correspond more to an isotropic distribution.

When computing the appropriate values for the energy dissipation it is not sufficient to include incoming electrons only. One must also add the backscattered electrons that are created when the incoming electrons ionise the neutral species. The influence made on the dissipation function by these backscattered electrons can be seen in Figure 5.1. The curves to the right of $x = 0$ represent energy dissipation due to incoming electrons, while the curves to the left of $x = 0$ are made up by backscattered electrons. To be able to do calculations with the effect of the backscattered electrons and the incoming electrons simultaneously we added the absolute values from the negative side with the positive values of s/R and came up with a new plot, shown in Figure 5.2.
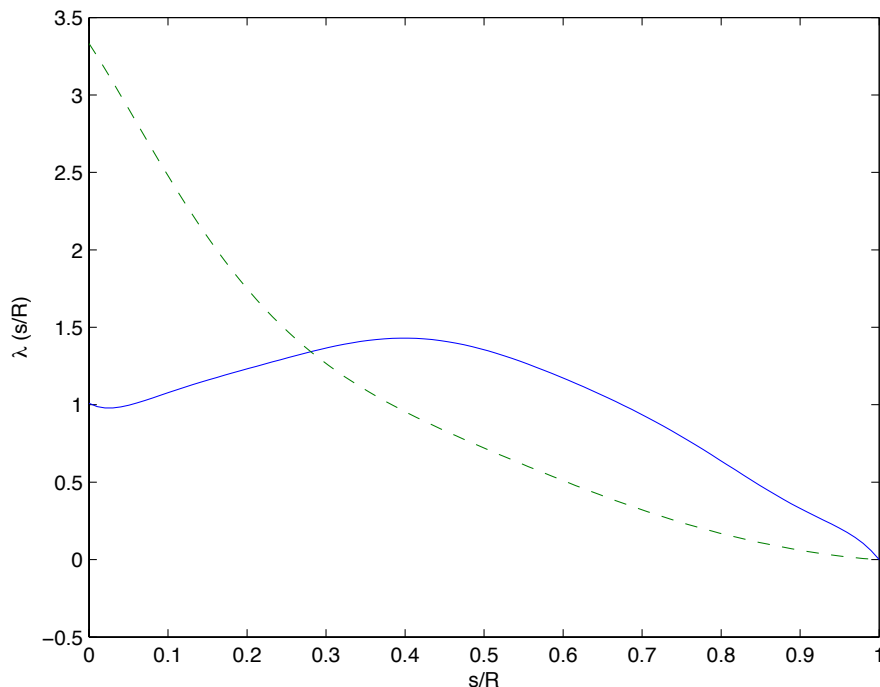
Figure 5.2: Energy dissipation for an isotropic distribution and a unidirectional beam – backscattered electrons included. The isotropic distribution is shown with a dashed line.

5.3   Numerical values

The incoming electrons are of many different energies, from thermal (a few eV) to several keV. In this report an energy range of 10 eV $< E <$ 2 keV has been considered. The electron flux can be calculated by knowing the velocity and the number of electrons at a given point. A velocity of roughly 100 km/s[1] combined with a number density of 0.1 electrons per square centimetre[2] implies an electron flux of about 10^6 cm^{-2} s^{-1}. The values for the mass density are derived from the neutral atmosphere, described in Section 4.1. With nitrogen being dominant, the mass density is based on the nitrogen mass density exclusively.

---

[1]Langmuir probe data, J.-E. Wahlund.
[2]Information from ELS, A. Coates.

5.4 Implementation

The ionisation rate is dependent on the electron flux, F, the electron energy, E, the energy dissipation function, $\lambda\left(\frac{s}{R}\right)$, the mass density, $\rho(z)$, the effective range, $R(E)$, and the energy loss per ion pair formation, $\triangle\varepsilon_{\text{ion}}$. Of these, only the electron flux and the electron energy are variable.[3] Figure 5.3 shows what a typical ionisation curve may look like, with the ionisation rate on the x–axis and the altitude on the y–axis.

For certain values of the energy and the flux, the ionisation rates reach a maximum at a given altitude, after which they quickly decrease. This is due to the fact that, for any given energy, each electron may only penetrate the atmosphere to a given depth. Given more energy, the electron may penetrate deeper, but when it reaches its maximum depth, nearly all the energy is consumed and the ionisation rate approaches zero. This process is called energy degradation in a collisional atmosphere. Changes in the energy values thus result in a corresponding change of the peak altitude, whereas a variation of the flux value gives rise to a change in the magnitude of the ionisation rate. Greater flux leads to a higher ionisation rate and vice versa. This is not perfectly true for all cases, especially not for very low values of energy, but it is useful to have in mind as a rule of thumb.

This report considers two angular distributions for the incoming electron stream: a unidirectional beam and an isotropic distribution between $0°$ and $80°$. As can be seen in Figure 5.3 the unidirectional distribution gives rise to a sharper distribution than does the isotropic distribution. This can be explained by the fact that a unidirectional distribution goes straight into the atmosphere at a certain angle, whereas an isotropic distribution covers a wider range of angles.

5.5 Ionisation rates at lower electron energies

To obtain ionisation rates for lower electron energies a model by Prof. Dirk Lummerzheim at the Geophysical Institute, University of Alaska, was used [13]. The model takes an arbitrary incident electron spectrum and propagates it into a neutral atmosphere. From that it obtains the excitation and ionisation rates as a function of altitude. The model is made for being used on Earth's neutral atmosphere, but as it is possible to obtain the ionisation rate as a function of column density, it may be applied to the Titan atmosphere as well.

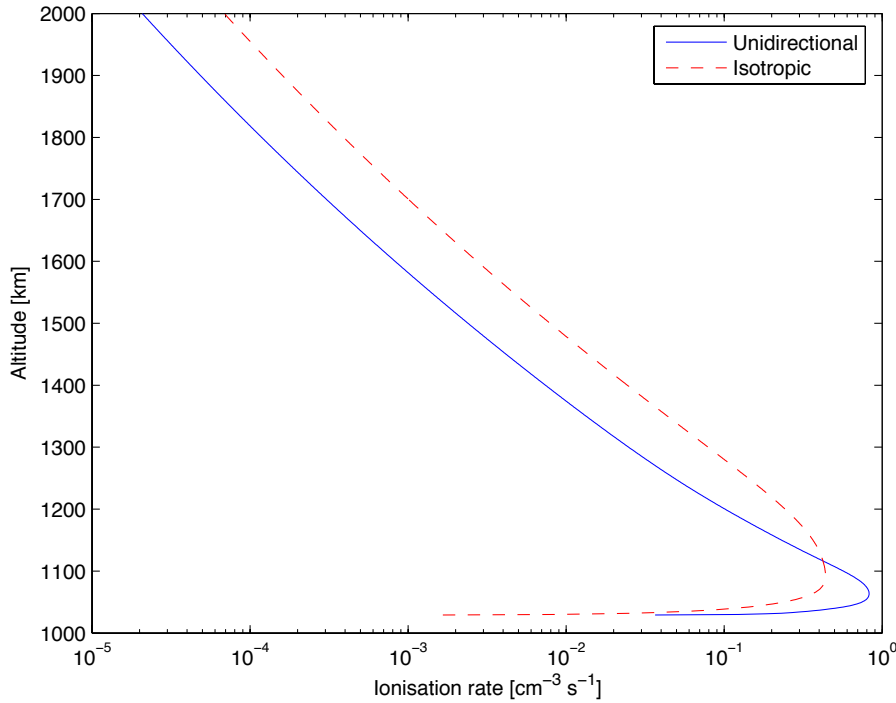[3]Which indirectly affects the effective range and consequently the energy dissipation.

Figure 5.3: Ionisation rates for a unidirectional and an isotropic distribution of the incoming electron stream. $E = 300$ eV and $F = 10^6$ cm^{-2} s^{-1}.

5.5.1 Properties of the model

The model code is written in Fortran 77 and the model is based on a transport calculation and solves an equation that describes how the electrons move through the neutral gas, loosing energy, producing secondaries in ionising collisions and scattering in angle. The transport equation solves for the electron intensity in a three dimensional parameter space: one spatial dimension, one for pitch angle and one in energy. As input the neutral density as a function of altitude and an arbitrary distribution of electrons are taken. The distribution of electrons is given in pitch angle and energy. The energy range for the electrons goes from thermal (fraction of an eV) to about 50 keV. In the model, the electrons are transported along a magnetic field into a volume of neutral density. Cross sections for N_2, O_2 and O are considered. The energy loss to ambient plasma is included by Coulomb collisions. The output from the model is put into binary data files which are read by IDL programs for plotting. There is also a human readable ASCII file produced. The output contains altitude, density, column

density, ionisation, dissociation and excitation rates of all background neutral species as a function of altitude, the various optical emission rates as function of altitude and the brightness of various emission features [13].

5.5.2   Using the model

As the ionisation rate given in Section 5.1 breaks down for electrons with an energy less than 200 eV, we need to use Lummerzheim's model [13] to obtain rates for electrons with energies below this threshold. The model cannot be used to simulate a mono-energetic electron beam, why a Gaussian distribution has to be used. The Gaussian distribution is constructed with the peak at a given energy and a half width of 10% of that energy. We used the model to get output data for electrons of 10, 20, 30, 40, 50, 70, 100, and 150 eV. By calculating the mass density for a given height in the neutral atmosphere, consisting of only N_2, we can use the model output to obtain the ionisation rates at the corresponding altitudes.

5.5.3   Combining the models

Our model gives ionisation rates for electrons of an energy of 200 or more eV. The model described above provides rates for energies lower than that. Knowing the ionisation rates for an energy spectra ranging from 10 eV to 2 keV, we may plot the maxima of the ionisation rates in the same figure for comparison. By doing that we may also compute the difference in flux between the two models. This can be done as we know the flux we use to achieve our results and we want a smooth changeover between the models. The upper plot in Figure 5.4 shows the ionisation maxima without having adjusted for the flux, whereas the lower plot shows the curves after having done the adjustment. The adjustment factor was found to be 1.5×10^{-4}. This is accounted for in the coming calculations.

Knowing the flux and the ionisation rates for the lower energies, we can show how the ionisation maxima in kilometres change with the electron energy. In Figure 5.5 the peak altitudes for ionisation rates of different energies of electrons are shown. At low energies the model of Prof. Lummerzheim [13] is used to calculate the rates, while at higher energies the rates is calculated as shown in Section 5.1. The low energy results seem coherent with the high energy ones.
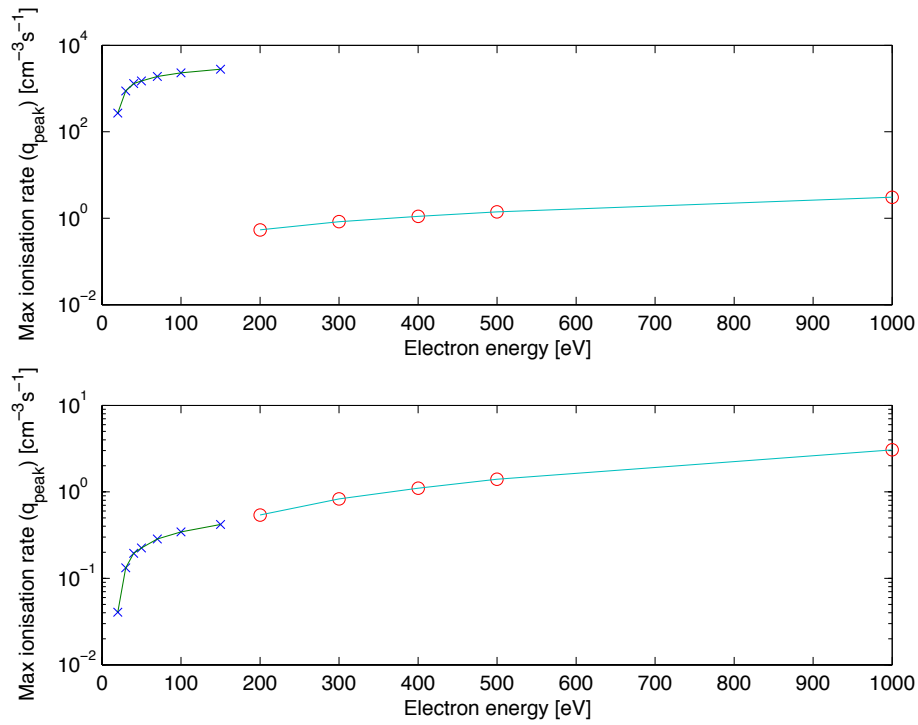
Figure 5.4: Ionisation maxima for various electron energies. Upper plot without adjustments for the flux and lower plot with adjustments made. The crosses show results derived from the model [13], the rings are given by the ionisation calculations in Section 5.1.
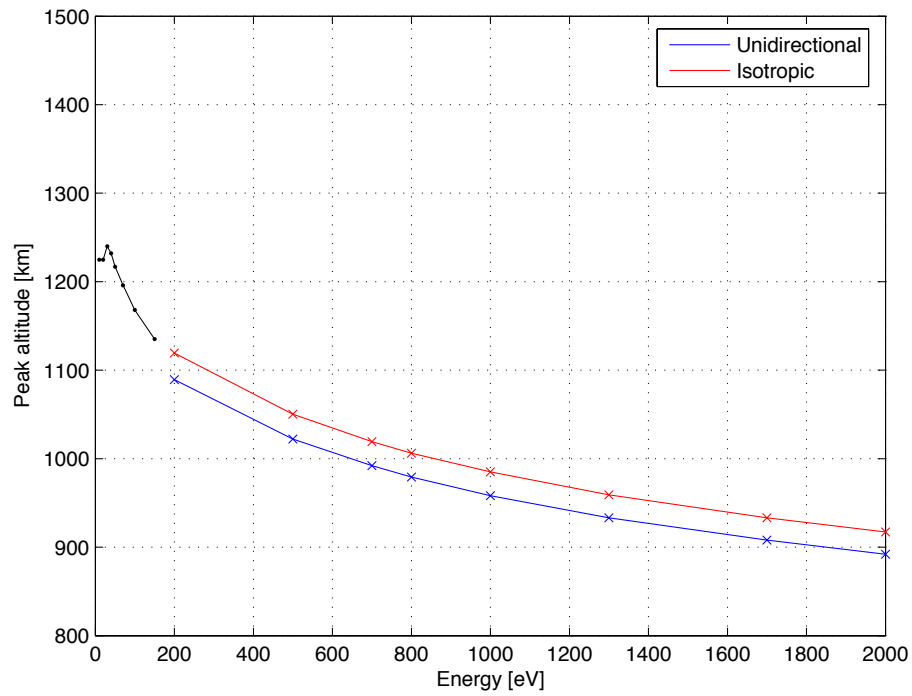
Figure 5.5: Peak altitudes for the ionisation rates. The black line shows results derived from the model [13], the red and blue are taken from the ionisation calculations in Section 5.1.

Chapter 6

Chemistry in Titan's ionosphere

Titan's rich atmosphere gives rise to a complex ionosphere. Many hundred chemical reactions take place simultaneously, of different relevance for the total ionisation level of the ionosphere. This work is focused on the ionisation of nitrogen and the dominant reactions that follow from that. Nitrogen is of certain interest as it is by far the most common constituent of the Titan atmosphere. Figure 6.1 illustrates the major production and loss channels in the chemistry of Titan's ionosphere. The major ion, $HCNH^+$, is mainly produced by the reactions showed by the shaded line. What is not shown in the flowchart is the fact that each of the molecular ion species do not exclusively react with other species. There is also always the possibility of the different species to recombine dissociatively. This is, however, not taken into consideration in the following calculations, except when clearly said so.

6.1 Ion chemistry

As seen in Figure 6.1 there are four reactions that are responsible for the primary production of $HCNH^+$. In the first step the nitrogen gets ionised by, in this case, magnetospheric electrons:

$$N_2 + e^{-*} \rightarrow N_2^+ + e^- + e^{-*}. \tag{6.1}$$

The rate of this reaction has been calculated in Chapter 5 and varies with the energy and the flux of the electrons. The peak production rate for an electron energy of 300 eV and a flux of 10^6 cm^{-2} s^{-1} was computed to be 0.8 cm^{-3}
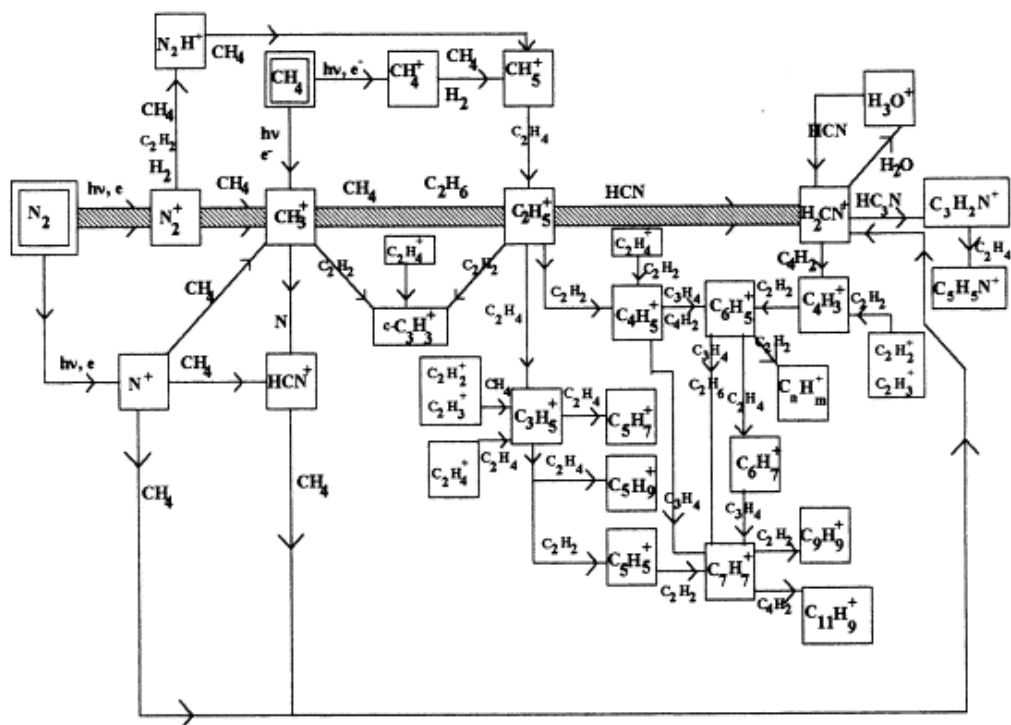
Figure 6.1: Flowchart representing the major ion chemistry in the ionosphere of Titan [14].

s^{-1}. For future references the production rate of (6.1) is labelled β. The ionised nitrogen reacts with neutral methane as

$$N_2^+ + CH_4 \rightarrow CH_3^+ + N_2 + H, \tag{6.2}$$

with a reaction rate of:

$k_{6.2} = 9.12 \times 10^{-10}$ cm^3 s^{-1} [14].

Further reactions involving CH_4 and HCN leads to the formation of HCNH$^+$. The nitrogen and HCN densities are given in Chapter 4, Sections 4.1 and 4.2 respectively.
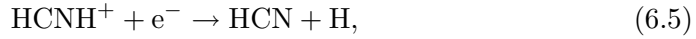
$$CH_3^+ + CH_4 \rightarrow C_2H_5^+ + H_2, \tag{6.3}$$
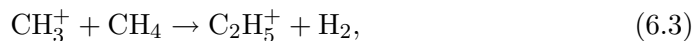
$k_{6.3} = 1.10 \times 10^{-9}$ cm^3 s^{-1} [14],

$$C_2H_5^+ + HCN \rightarrow HCNH^+ + C_2H_4, \tag{6.4}$$
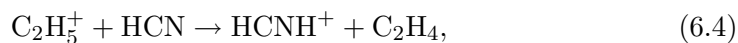
$k_{6.4} = 2.70 \times 10^{-9}$ cm^3 s^{-1} [14].

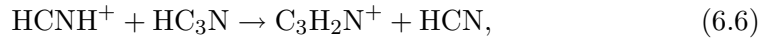The major loss channel for HCNH$^+$ is the electron dissociative recombination reaction:

$$\text{HCNH}^+ + \text{e}^- \rightarrow \text{HCN} + \text{H}, \qquad (6.5)$$

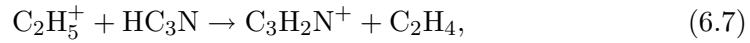$\alpha_1 = 6.40 \times 10^{-7}(300/T_\text{e})^{1/2}$ cm^3 s^{-1} [14].

α_1 is dependent on the electron temperature, which for all further calculations has been set to 700 K, as measured by the Langmuir probe (see Figure 7.1, page 44).

6.2 Higher mass nitrile species

Beside the four main reactions listed above there are several other reactions taking place simultaneously. In the following equations, the concentration of HCNH$^+$ is considered to be constant. This assumption can be done, as the density of HCNH$^+$ is greater than the other ion densities by orders of magnitude, and therefore can be considered constant in comparison. C$_3$H$_2$N$^+$ is formed via the reactions:

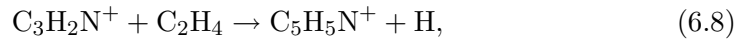$$\text{HCNH}^+ + \text{HC}_3\text{N} \rightarrow \text{C}_3\text{H}_2\text{N}^+ + \text{HCN}, \qquad (6.6)$$

$k_{6.6} = 3.40 \times 10^{-9}$ cm^3 s^{-1} [14],

$$\text{C}_2\text{H}_5^+ + \text{HC}_3\text{N} \rightarrow \text{C}_3\text{H}_2\text{N}^+ + \text{C}_2\text{H}_4, \qquad (6.7)$$

$k_{6.7} = 3.55 \times 10^{-9}$ cm^3 s^{-1} [14],

and lost mostly in the reaction:

$$\text{C}_3\text{H}_2\text{N}^+ + \text{C}_2\text{H}_4 \rightarrow \text{C}_5\text{H}_5\text{N}^+ + \text{H}, \qquad (6.8)$$

$k_{6.8} = 1.30 \times 10^{-9}$ cm^3 s^{-1} [14],

where the density of HC$_3$N and C$_2$H$_4$ is obtained from the Toublanc and Yung models [6, 7, 8]. Currently there is no species known which is believed to react with C$_5$H$_5$N$^+$ leaving it no loss channel except electron dissociative recombination [14]:

$$\text{C}_5\text{H}_5\text{N}^+ + \text{e}^- \rightarrow \text{C}_5\text{H}_5\text{N}, \qquad (6.9)$$
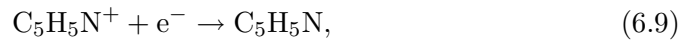
$\alpha_2 = 6.40 \times 10^{-7}(300/T_e)^{1/2}$ cm^3 s^{-1} [14].

We use the same rate for this reaction as we did for HCNH$^+$. The dissociative recombination rate coefficients for these species are about the same. The electron density is the sum of all the ion densities. There is an electron density uncertainty due to this effect of $\approx$10% or less [15].

6.3   Ion density calculations

The equation of continuity for number densities, n,

$$\frac{\partial n}{\partial t} + \nabla(n\bar{v}) = \sum Q - L \tag{6.10}$$

conserves the number of particles in a system. The source term, Q, and the loss term, L, are equal for chemical equilibrium. Also, since the velocity, $\bar{v}$, is very small in this context the transport term, $\nabla(n\bar{v})$, can be neglected[1] and Equation (6.10) can be simplified into:

$$\frac{\partial n}{\partial t} = \sum Q - L. \tag{6.11}$$

Subsequently Equations (6.1) and (6.2) can be combined into:

$$\frac{\partial n(N_2^+)}{\partial t} = \beta - k_{6.2}n(N_2^+)n(CH_4). \tag{6.12}$$

The same applies to Equations (6.3) – (6.9) which gives rise to the new equations

$$\frac{\partial n(CH_3^+)}{\partial t} = k_{6.2}n(N_2^+)n(CH_4) - k_{6.3}n(CH_3^+)n(CH_4), \tag{6.13}$$

$$\frac{\partial n(C_2H_5^+)}{\partial t} = k_{6.3}n(CH_3^+)n(CH_4) - k_{6.4}n(C_2H_5^+)n(HCN) \tag{6.14}$$

and

$$\frac{\partial n(H_2CN^+)}{\partial t} = k_{6.5}n(C_2H_5^+)n(HCN) - \alpha_1 n(H_2CN^+)n_{e_1}. \tag{6.15}$$

Charge quasineutrality requires

---

[1]Below an altitude of 1400 km.

$$n_{e_1} \approx n(C_2H_5^+) + n(H_2CN^+), \tag{6.16}$$

as these two ions are dominant in comparison to the others. Further;

$$\frac{\partial n(C_3H_2N^+)}{\partial t} = k_{6.6}n(H_2CN^+)n(HC_3N) + k_{6.7}n(C_2H_5^+)n(HC_3N) - k_{6.8}n(C_3H_2N^+)n(C_2H_4) \tag{6.17}$$

and

$$\frac{\partial n(C_5H_5N^+)}{\partial t} = k_{6.8}n(C_3H_2N^+)n(C_2H_4) - \alpha_2 n(C_5H_5N^+)n_{e_2} \tag{6.18}$$

with

$$n_{e_2} = n(N_2^+) + n(CH_3^+) + n(C_2H_5^+) + n(H_2CN^+) + n(C_3H_2N^+) + n(C_5H_5N^+). \tag{6.19}$$

In these calculations all the ions are added together to give a value of the total electron density. Every ion produced contribute to an increase of the electron density. The contribution of H_2CN^+ and $C_2H_5^+$ are still the most important, but we include the other ions to get a complete picture. As we assume equilibrium on Titan all the Equations (6.12) to (6.18) are set to be $= 0$. This means they can all be solved by reorganising and inserting the known values. From that follows:

$$n(N_2^+) = \frac{\beta}{k_{6.2}n(CH_4)}, \tag{6.20}$$

$$n(CH_3^+) = \frac{k_{6.2}n(N_2^+)}{k_{6.3}}, \tag{6.21}$$

$$n(C_2H_5^+) = \frac{k_{6.4}n(CH_3^+)n(CH_4)}{k_{6.4}n(HCN)}, \tag{6.22}$$

$$n(H_2CN^+) = \frac{k_{6.5}n(C_2H_5^+)n(HCN)}{\alpha_1 n_{e_1}}, \tag{6.23}$$

$$n(C_3H_2N^+) = \frac{k_{6.6}n(H_2CN^+)n(HC_3N) + k_{6.7}n(C_2H_5^+)n(HC_3N)}{k_{6.8}n(C_2H_4)}, \tag{6.24}$$

$$n(C_5H_5N^+) = \frac{k_{6.8}n(C_3H_2N^+)n(C_2H_4)}{\alpha_2 n_{e_2}}. \tag{6.25}$$

The density of the different ion species are dependent on the density of the ion species in the previous equation. Starting with Equation (6.20), which can easily be solved by inserting the production rate for N_2^+ and the density of methane, we solve all Equations (6.20) – (6.25). All the ion densities and the electron density can later be plotted together for illustration and comparison. Figures 6.2 and 6.3 show the relationship between the ionisation rates and the two electron densities.[2] In Figures 6.4, 6.5, 6.6 and 6.7 all ion species and the total electron density are shown for a given electron energy and flux. The first two representing an isotropic distribution and the second two a unidirectional beam. These four figures can be compared with Figure 6.8, which show the actual densities of the species measured by INMS in the Titan ionosphere. What should be noticed is the cross-over at approximately 1450 km between H_2CN^+ and $C_2H_5^+$. The actual data model show that the two curves approach each other at an altitude of 1450 km, with the actual cross-over appearing at 1550 km. This cross-over can be seen in all five figures at approximately the same altitude, which gives an indication to that the model is correct. One may, however, note that the model based on the unidirectional beam shows better agreement to the actual data, than does the isotropic distribution. This is most clearly seen by looking at the altitudes for the cross-overs in the five figures. This observation leads us to the decision to concentrate on the unidirectional beam for further calculations. The heavy ions, e.g. $C_5H_5N^+$ and $C_3H_2N^+$, are quite common at low altitudes, after which they quickly diminish in density and lose importance for the total electron density. By comparing the Yung and the Toublanc model to the actual data model, we can determine that the Toublanc model shows better agreement to observations and is therefore used in the continuation.

---

[2]Based on models by Toublanc and Yung.
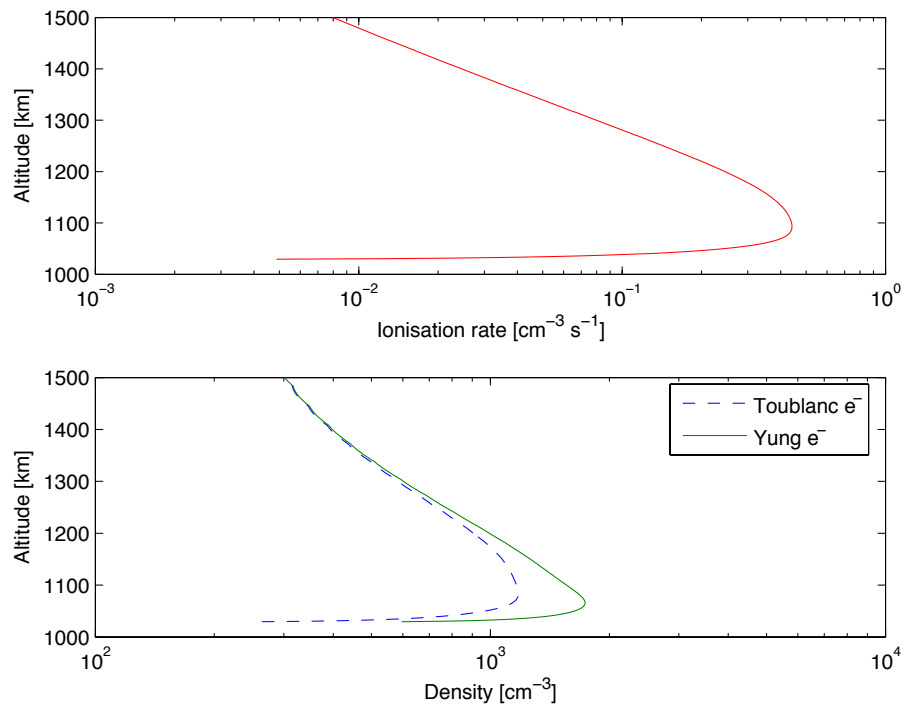
Figure 6.2: The ionisation rate (upper plot) and electron density given for an isotropic distribution. $E = 300$ eV and $F = 10^6$ cm^{-2} s^{-1}.
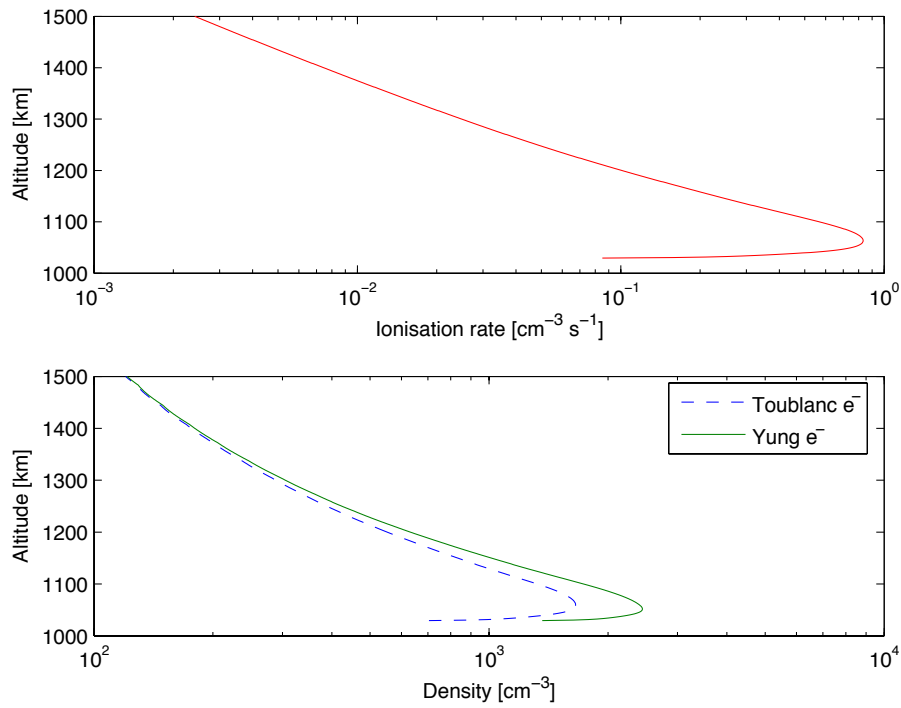
Figure 6.3: The ionisation rate (upper plot) and electron density given for a unidirectional beam. $E = 300$ eV and $F = 10^6$ cm^{-2} s^{-1}.
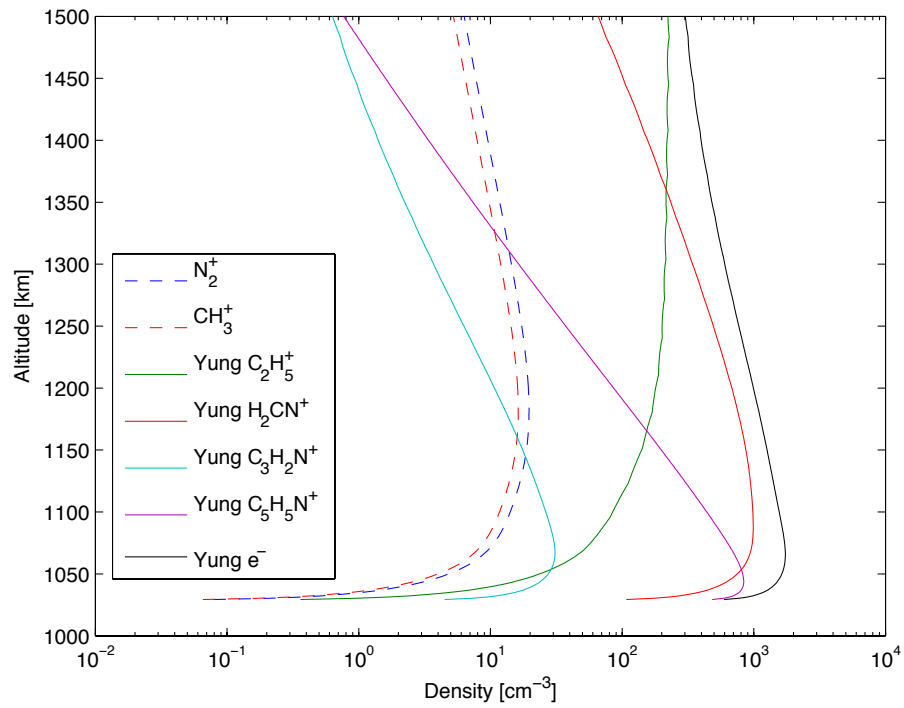
Figure 6.4: Ion densities based on the Yung model [7, 8] given for an isotropic distribution. $E = 300$ eV and $F = 10^6$ cm^{-2} s^{-1}.
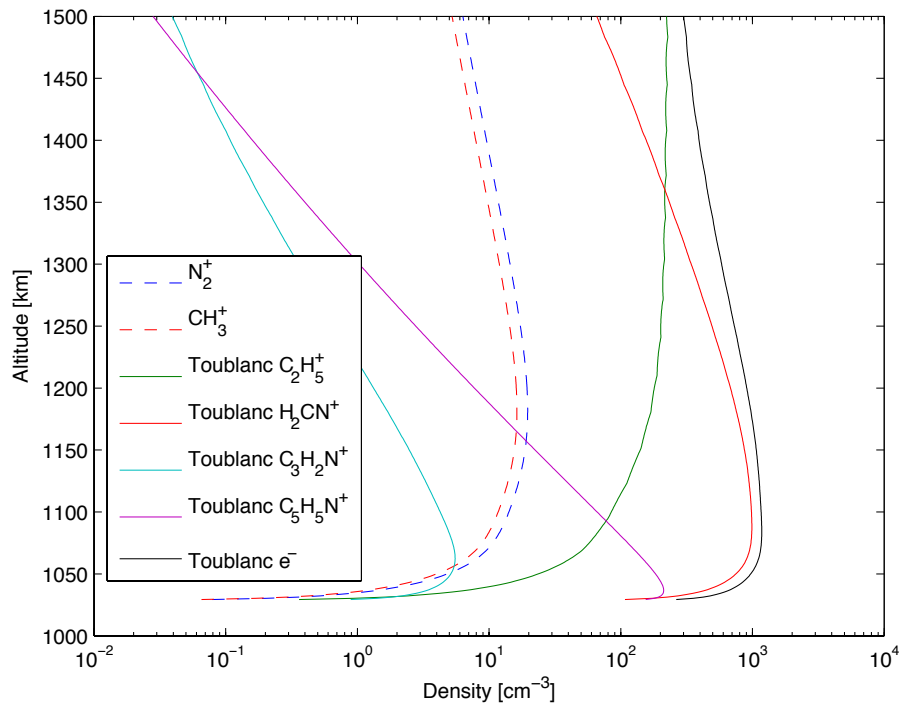
Figure 6.5: Ion densities based on the Toublanc model [6] given for an isotropic distribution. $E = 300$ eV and $F = 10^6$ cm^{-2} s^{-1}.

Figure 6.6: Ion densities based on the Yung model [7, 8] given for a unidirectional beam. $E = 300$ eV and $F = 10^6$ cm^{-2} s^{-1}.

Figure 6.7: Ion densities based on the Toublanc model [6] given for a unidirectional beam. $E = 300$ eV and $F = 10^6$ cm^{-2} s^{-1}.
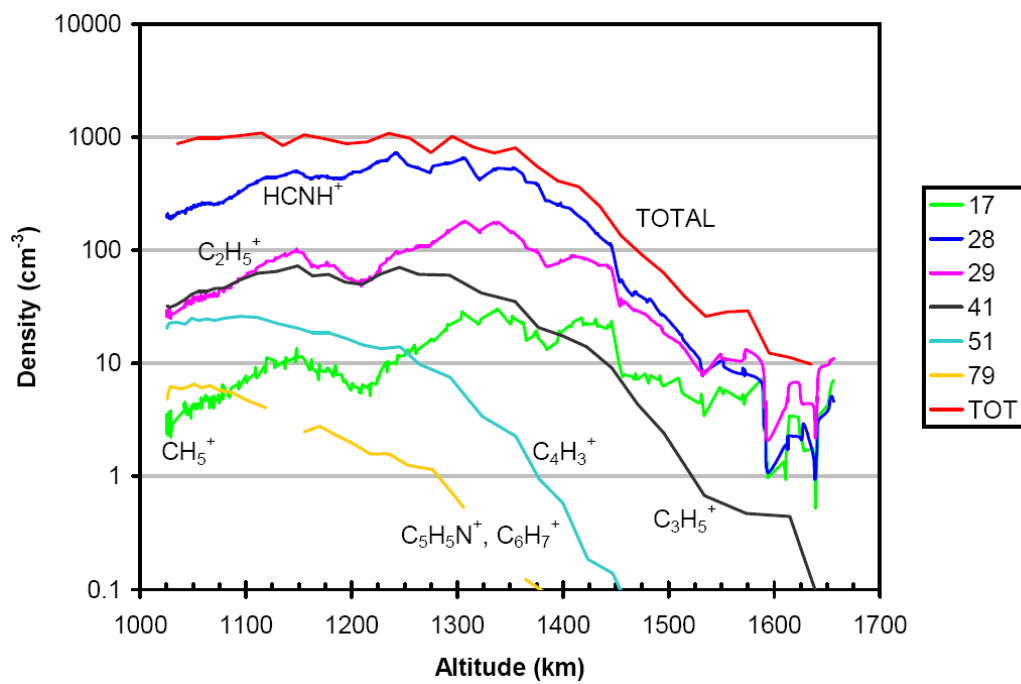
Figure 6.8: Ion densities from INMS data. 'Total' is equivalent to the electron density [16].

CHAPTER 7

ELECTRON SPECTRUM
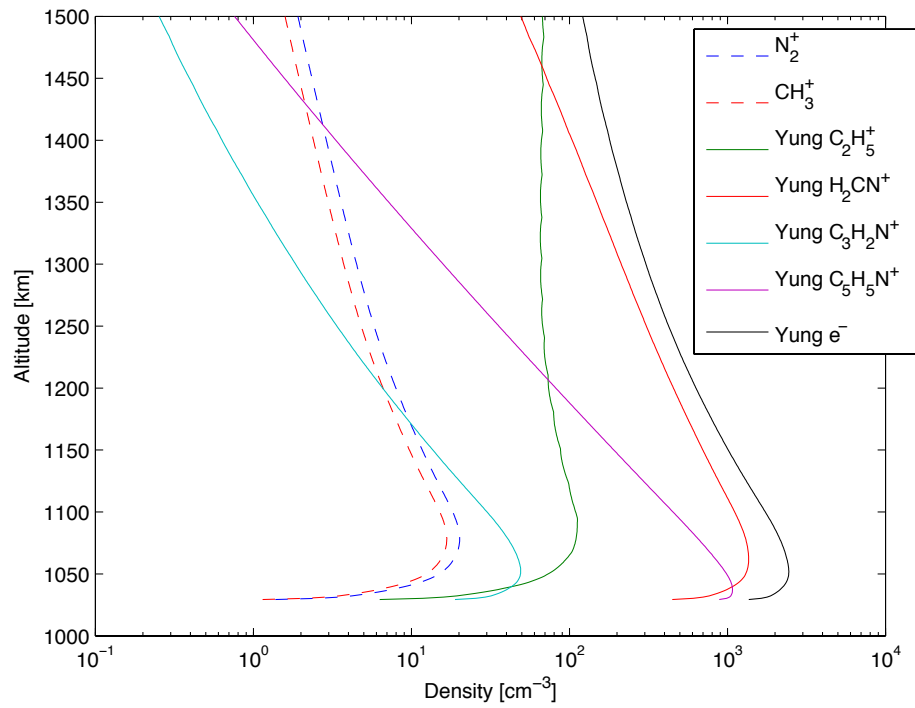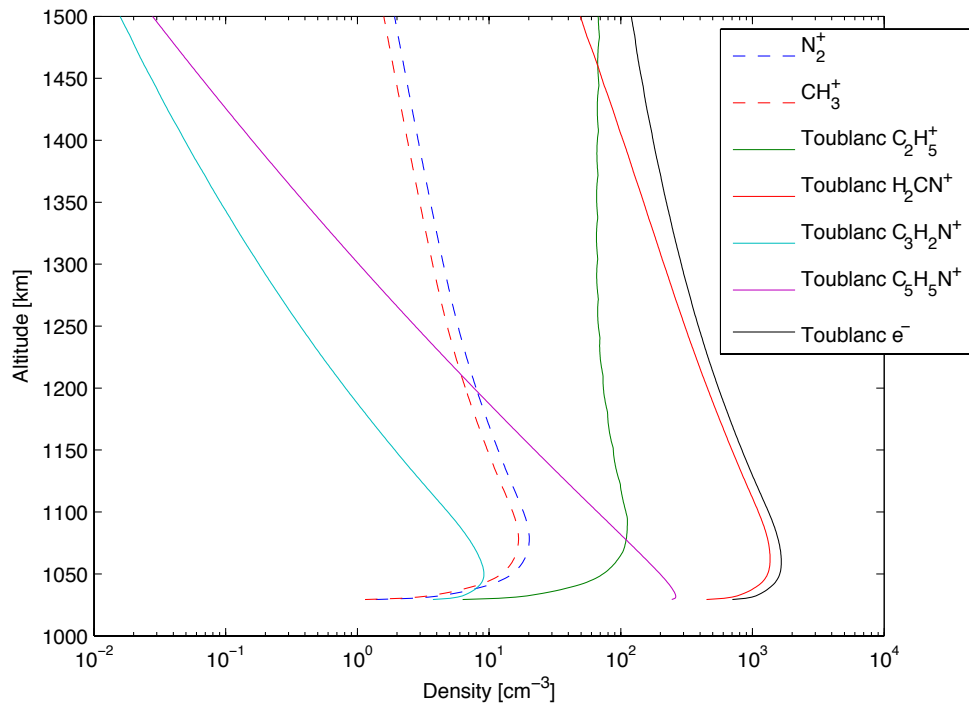
The main aim of this report is to try to find an energy spectrum of the incoming electrons into the ionosphere of Titan. This is done by looking at the electron densities measured by the Langmuir probe on Cassini. Using our model for Titan's ionosphere, described in Chapter 6, we may use the results of the ionisation calculations performed in Chapter 5 to calculate electron densities for electron streams of varying flux and energy. The final step is to present a spectrum of electrons of various flux and energy that put together will form the in situ measured density profile.

7.1   Electron density measured by Cassini

The electron density near Cassini is measured by the Langmuir probe (The basic theory of how it works is presented in Chapter 3.1.1 on page 8). At the same time, the electron temperature and the averaged ion mass are derived.[1] These three parameters are displayed in Figure 7.1. The values for the inbound track are shown in red and the outbound in black. Only the outbound track was chosen for comparison, since the inbound track partly occurred in sunlight. They are, nevertheless, almost similar for low values of altitude. Removing the inbound track and the values for very high altitudes we get a density curve that is shown in Figure 7.2. This data set is chosen for the model comparison.

7.2   Results

We try to obtain an electron spectrum by first looking at the density at the lowest altitude. The model is used to find an ionisation curve that has an electron

---

[1]The electron temperature and the averaged ion mass values are still preliminary.

Cassini RPWS LP, Inbound(red), Outbound(black)
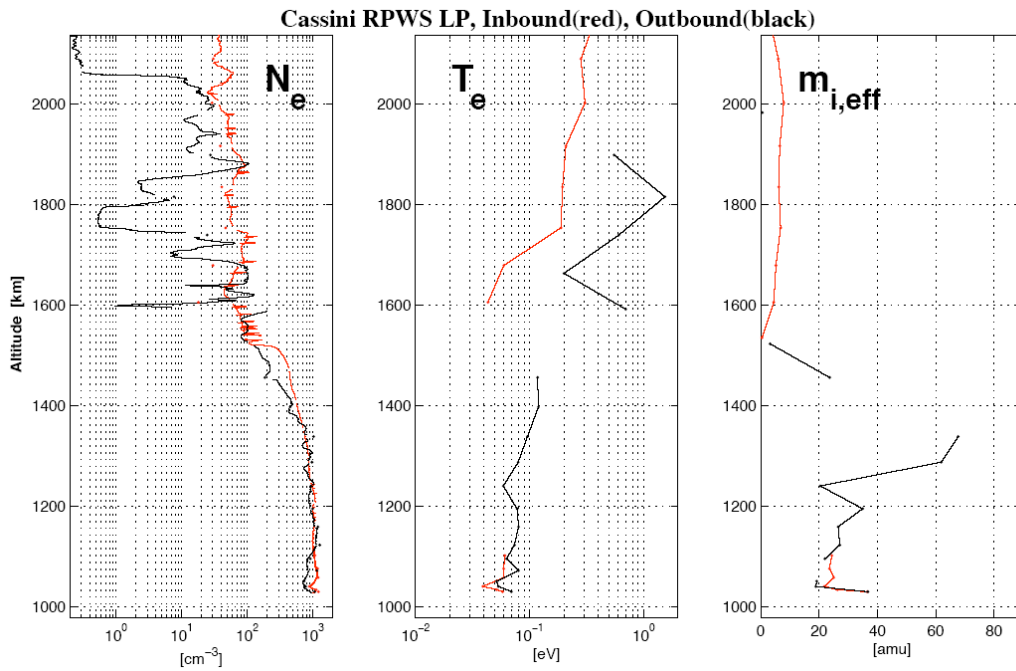
Figure 7.1: Parameters determined by the Langmuir probe, T5 flyby, April 16, 2005. Courtesy of J.-E. Wahlund.

density maximum that coincide with that density. An electron energy of 445 eV with a flux of 1.5×10^5 cm^{-2}s^{-1} is found to give a good agreement. After this we look at density profiles corresponding to successively lower energies. This includes density profiles that correspond to the different energies that was modelled by Prof. Lummerzheim (10, 20, 30, 40, 50, 70, 100 and 150 eV) [13]. As we only obtain the output data from those, we can only look at fixed energies, but the flux may still be varied. The best fit is reached by using the electron density models for $E = 150$ eV and $E = 30$ eV. The fluxes are 3×10^5 and 1×10^5 cm^{-2}s^{-1} respectively. Figure 7.3 shows the calculated profiles plotted next to the real density profile.

7.2.1   Comparison with CAPS data

Figure 7.4 shows the electron energy distribution at various pitch angles and for various times. The data is taken from the CAPS instrument package and is not calibrated. This means that the detection of the electrons is given in counts, and not in flux. There is, nevertheless, a relation between the two. More counts do correspond to a greater flux for a given energy, but the relation is not strictly
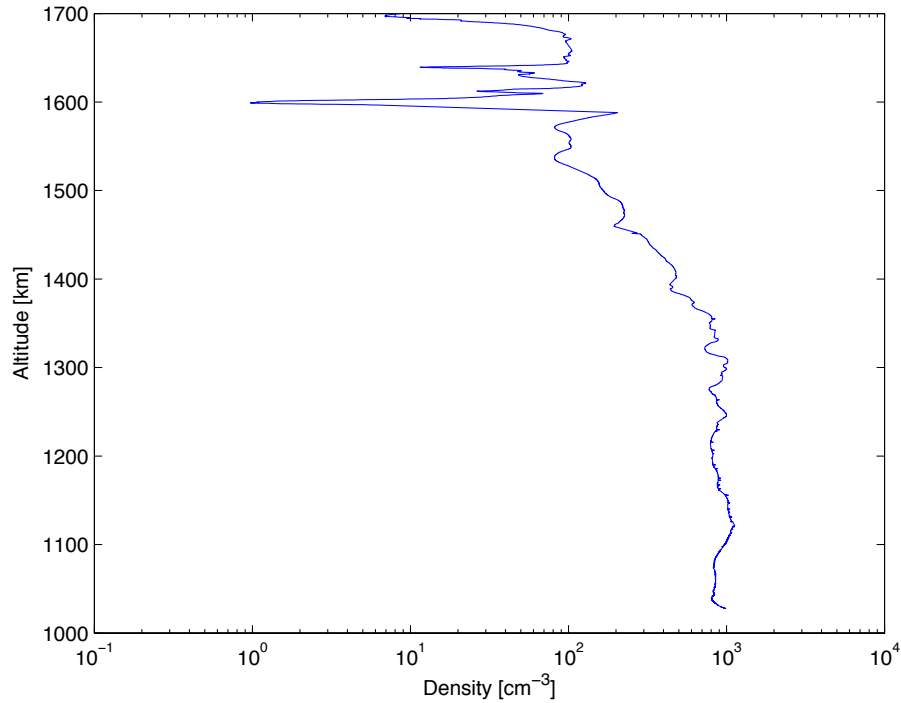
Figure 7.2: The electron density measured by the Langmuir probe, T5 flyby, April 16, 2005. Outbound track.

linear. We may therefore consider the energies of the electrons, whereas the exact flux is yet to be calculated. The wake just after 19 h is due to the passing of Titan. What we have looked into is the region right after that, where the incoming electrons are shown for the outbound track. Excluding the photoelectrons, that can be seen as a constant count at low electron energies, we end up with incoming electrons in a range of a few tens to approximately 500 eV. This is the same range as we achieved using our model, which is a good indication to that the model is correct and can well be used.

7.2.2 Discussion

Before starting to derive the electron energy spectrum, we expected it to be composed of many profiles that all correspond to a certain energy and a certain flux. However, this approach had to be discarded since only three profiles were enough to account for the electron density as a function of altitude. Instead, one need to model an energy spectrum $N(E)\mathrm{d}E$, see page 50. What can be
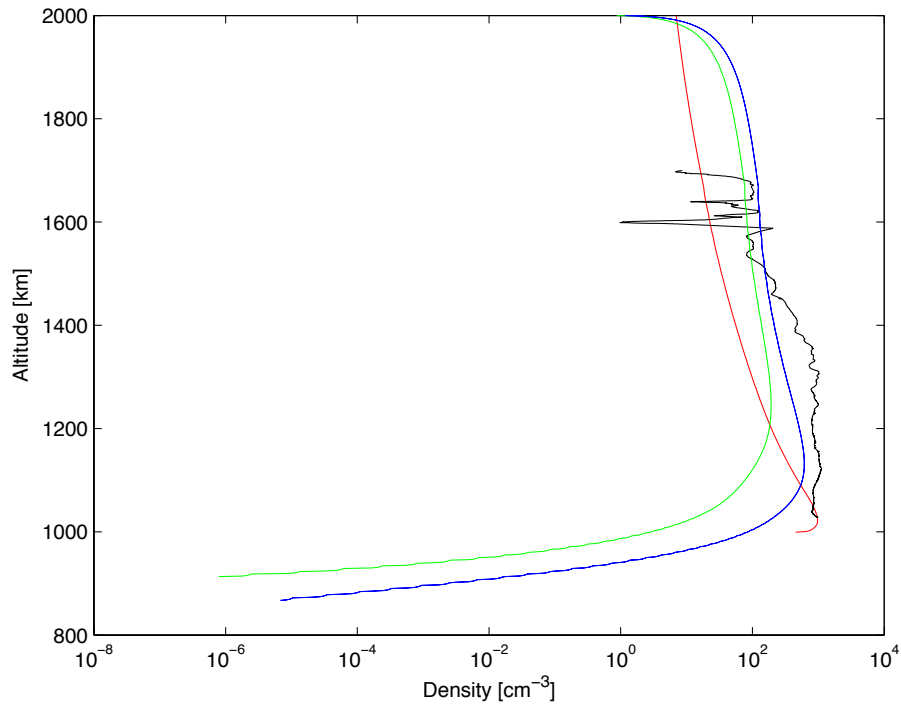
Figure 7.3: Electron densities for energy values of 30 eV (shown in green), 150 eV
(blue) and 445 eV (red) next to the actual electron density measured on Titan
(black).

established with our approach is that the upper limit for the electron energy
to fit the measured density is around 450 eV. Furthermore, we have shown that
electrons within the energy range 30–450 eV can account for the observed electron
density and ion composition altitude profiles.
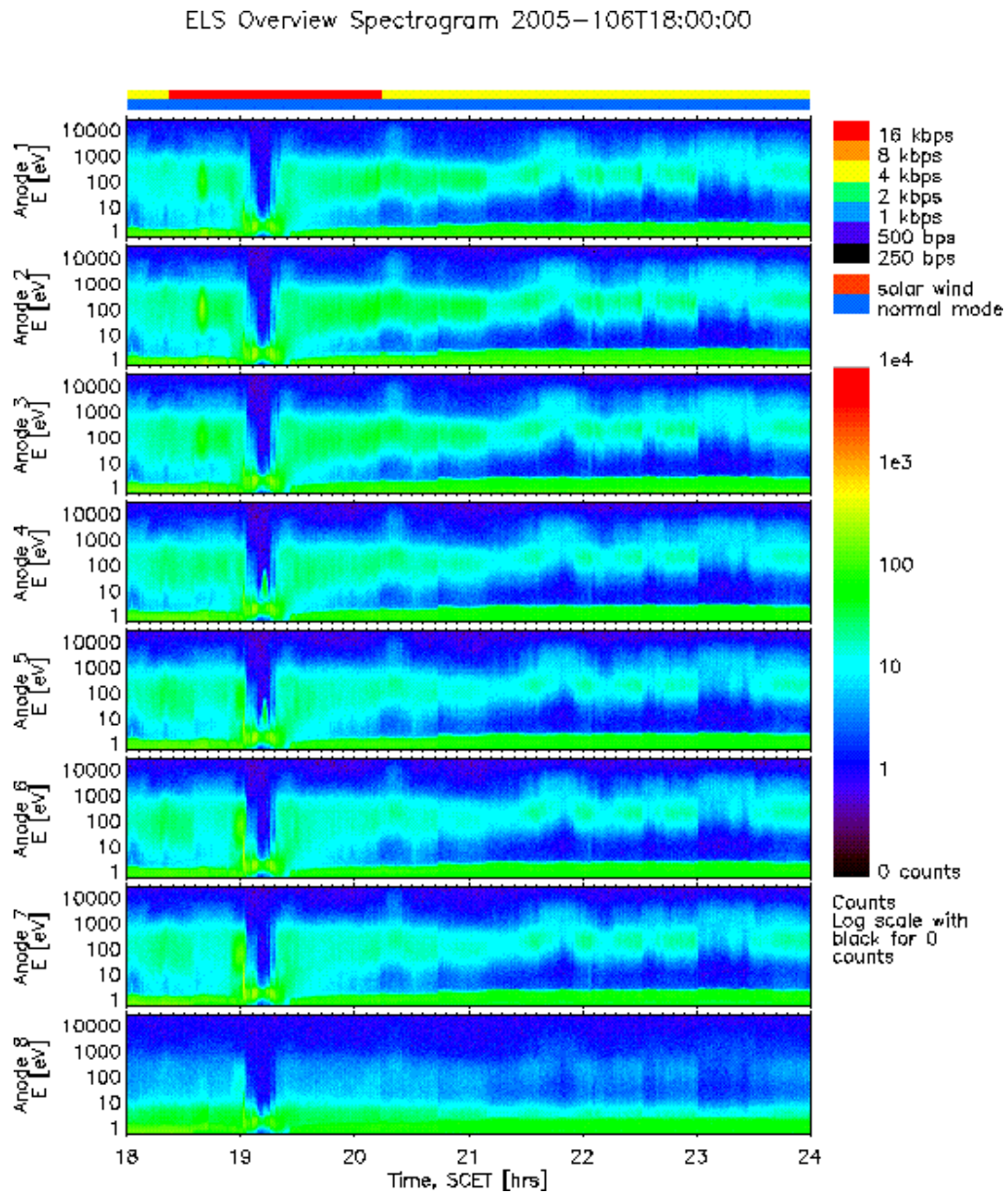
Figure 7.4: CAPS ELS data. Figure from Gethyn Lewis and Andrew Coates.

CHAPTER 8

CONCLUSION AND OUTLOOK

We conducted this study to investigate whether magnetospheric electrons could be the main source of ionisation of the atmosphere in eclipse. To be able to accomplish this, we made a number of suitable assumptions:

- We used various models of the Titan neutral atmosphere in order to put together our own model consisting of the species that were needed for further calculations. The models we used were based on newly performed measurements from Cassini[1] as well as over 20 years old data from the Voyager spacecraft.[2]

- We looked at two angular distributions of the incoming electron stream: a unidirectional beam and an isotropic distribution. None of these are equivalent to the actual distribution observed on Titan, but the unidirectional beam proved to be a better assumption.

- Regarding the ion chemistry we looked at the main reactions only – ignoring hundreds of less common reactions. We would get a more complete picture by including all possible reactions, but that would not be feasible, as we still do not know exactly how the chemical reactions behave on Titan. Even if we did know the exact chemistry of Titan, we do believe that the reactions chosen are so important that the others may be ignored to a first approximation.

With these assumptions, we came to the conclusion that magnetospheric impacting electrons alone can account for the observed density and composition profiles with altitude.

---

[1]Yelle and Müller–Wodarg.
[2]Yung and Toublanc.

Alternative approach

This report is based on Equation (5.3) for the ionisation rate,

$$q(z) = \frac{FE\lambda\left(\frac{s}{R}\right)\rho(z)}{R(E)\,\triangle\,\varepsilon_{\text{ion}}}.$$

We assumed a monoenergetic beam and performed individual calculations for electrons of different energies. These equations may be convolved with any arbitrary energy spectrum to obtain energy ionisation rates for model spectra. A distribution of the form

$$N(E)\mathrm{d}E = E^{\gamma}e^{(-E/E_0)}\mathrm{d}E \tag{8.1}$$

could be used to represent different spectra. An appropriate choice of the parameters γ and E_0 yields power laws, exponential variations or Maxwellian distributions [11]. Inserting this into the given equation for the ionisation rate we obtain

$$q(z) = \int_0^\infty q(z, E)N(E)\mathrm{d}E. \tag{8.2}$$

We have, however, not yet carried out this approach here. Doing that could be considered as a possible extension of this work.

ACKNOWLEDGEMENTS

Appendix A

Titan HCN

Table A.1: Titan GCM globally averaged output.

Ht (km)	Pres (nbar)	Temp (K)	HCN (cm-3)
621.502	98.5370	161.094	3.68193e+07
642.983	66.0514	158.898	3.72162e+07
664.523	44.2755	157.570	3.71318e+07
686.215	29.6788	156.849	3.68136e+07
708.134	19.8943	156.611	3.63866e+07
730.340	13.3355	156.630	3.59387e+07
752.854	8.93908	156.596	3.55124e+07
775.658	5.99204	156.259	3.50444e+07
798.706	4.01659	155.526	3.42701e+07
821.946	2.69240	154.456	3.27771e+07
845.344	1.80477	153.202	3.02814e+07
868.889	1.20977	151.947	2.68327e+07
892.600	0.810935	150.860	2.27731e+07
916.520	0.543586	150.056	1.85546e+07
940.710	0.364377	149.594	1.45712e+07
965.238	0.244249	149.475	1.10790e+07
990.172	0.163725	149.665	8.19376e+06
1015.58	0.109748	150.095	5.92243e+06
1041.51	0.0735664	150.685	4.20281e+06
1068.00	0.0493130	151.349	2.94015e+06
1095.10	0.0330555	152.020	2.03438e+06
1122.84	0.0221578	152.655	1.39581e+06

Ht (km)	Pres (nbar)	Temp (K)	HCN (cm-3)
1151.23	0.0148528	153.226	951370.
1180.30	0.00995612	153.726	644978.
1210.10	0.00667379	154.151	435260.
1240.66	0.00447357	154.507	292502.
1272.04	0.00299873	154.801	195752.
1304.30	0.00201011	155.041	130430.
1337.55	0.00134741	155.234	86480.0
1371.89	0.000903199	155.387	57011.4
1407.49	0.000605432	155.506	37325.1
1444.54	0.000405833	155.598	24228.2
1483.34	0.000272038	155.666	15557.1
1524.28	0.000182353	155.713	9849.93
1567.94	0.000122235	155.743	6120.92
1615.20	8.19363e-05	155.758	3707.31
1667.43	5.49236e-05	155.758	2164.82

Appendix B

Matlab routines

B.1 Major neutral constituents

B.1.1 atm.m

```
1   %%%%%%%%%%%%%%%%%%%%%%%%%%%%%%%%%%%%%%%%%%%%%%%%%%%%%%%%%%%%%%%%%%%%%%%%%%%%%%%%
2   %
3   %  atm.m
4   %
5   %  The neutral atmosphere
6   %
7   %  Karin Agren, Swedish Institute of Space Physics, Uppsala, 2005.
8   %%%%%%%%%%%%%%%%%%%%%%%%%%%%%%%%%%%%%%%%%%%%%%%%%%%%%%%%%%%%%%%%%%%%%%%%%%%%%%%%
9
10  % Values taken from INMS T5 data
11
12  % Heights
13  x_N2 = [1000 1010 1025 1070 1130 1230 1310 1385 1470 1560 1670 1720 1765 ...
14      1810 1970 1985]';
15  x_CH4 = [1050 1135 1185 1250 1365 1510 1600 1720 1840 1950]';
16  x_H2 = [1020 1065 1165 1210 1270 1365 1480]';
17
18  % Densities
19  N_N2 = [5e9 4e9 3e9 2e9 1e9 3e8 1e8 3e7 1e7 3e6 1e6 6e5 4e5 3e5 1e5 8e4]';
20  N_CH4 = [6e7 3e7 2e7 1e7 2e6 1e6 6e5 3e5 2e5 1.3e5]';
21  N_H2 = [2e7 1e7 3e6 2e6 1e6 6e5 4e5]';
22
23  % Finding the appropriate equations
24
25  xt_N2 = log(x_N2);
26  Nt_N2 = log(N_N2);
27  A_N2 = [xt_N2.^0 xt_N2.^1];
28  a_N2 = A_N2\Nt_N2;
29
30  xt_CH4 = log(x_CH4);
31  Nt_CH4 = log(N_CH4);
32  A_CH4 = [xt_CH4.^0 xt_CH4.^1];
33  a_CH4 = A_CH4\Nt_CH4;
34
35  xt_H2 = log(x_H2);
36  Nt_H2 = log(N_H2);
37  A_H2 = [xt_H2.^0 xt_H2.^1];
```

```
38   a_H2 = A_H2\Nt_H2;
39
40   % Plot
41
42   xm = linspace(0, 2000);
43   xm_H2 = linspace(0, 1470);
44   Nm_N2 = exp(a_N2(1))*xm.^a_N2(2);
45   Nm_CH4 = exp(a_CH4(1))*xm.^a_CH4(2);
46   Nm_H2 = exp(a_H2(1))*xm_H2.^a_H2(2);
47   z_H2 = [1470 2000];
48   w_H2 = [3e5 3e5];
49   semilogx (Nm_N2,xm,'--',Nm_CH4,xm,'-',Nm_H2,xm_H2,'r-.',N_N2,x_N2,'+',...
50       N_CH4,x_CH4,'o',N_H2,x_H2,'x',w_H2,z_H2,'r-.')
51
52   xlabel('density [cm-3]')
53   ylabel('altitude [km]')
54   legend('N2', 'CH4', 'H2')
55
56   % Save data
57
58   save atm a_N2 a_CH4 a_H2;
59
60
```

B.2 Energy dissipation

B.2.1 dep.m

```
1   %%%%%%%%%%%%%%%%%%%%%%%%%%%%%%%%%%%%%%%%%%%%%%%%%%%%%%%%%%%%%%%%%%%%%%%%%%%%%%%%
2   %
3   %  dep.m
4   %
5   %  Energy dissipation
6   %
7   %  Karin Agren, Swedish Institute of Space Physics, Uppsala, 2005.
8   %%%%%%%%%%%%%%%%%%%%%%%%%%%%%%%%%%%%%%%%%%%%%%%%%%%%%%%%%%%%%%%%%%%%%%%%%%%%%%%%
9
10  % Values taken from Rees - including the backscattering
11
12  % s/R
13
14  N_uni = [0 0.05 0.1 0.15 0.2 0.3 0.4 0.5 0.6 0.7 0.8 0.9 1.0]';
15  N_iso = [0 0.01 0.05 0.1 0.15 0.2 0.3 0.4 0.5 0.6 0.7 0.8 0.9 1.0]';
16
17  % lambda s/R
18
19  x_uni = [1.01 0.99 1.09 1.15 1.23 1.37 1.43 1.35 1.18 0.93 0.64 0.33 0]';
20  x_iso = [3.28 3.33 2.88 2.47 2.11 1.74 1.26 0.96 0.72 0.51 0.32 0.17 0.06...
21      0]';
22
23  % Finding the appropriate equations
24
25  p_uni = polyfit(N_uni,x_uni,9);
26  p_iso = polyfit(N_iso,x_iso,8);
27
28  % Plot
29
30  z_uni = linspace(0,1);
31  z_iso = linspace(0,1);
32  q_uni = polyval(p_uni,z_uni);
33  q_iso = polyval(p_iso,z_iso);
34  plot(z_uni,q_uni,'-',N_uni,x_uni,'o',z_iso,q_iso,'--',N_iso,x_iso,'+')
35
36  xlabel('s/R')
37  ylabel('\lambda s/R')
38
39  % Save data
40
41  save dep p_uni p_iso
42
```

B.3   Minor neutral constituents

B.3.1   HC3N.m

```
1   %%%%%%%%%%%%%%%%%%%%%%%%%%%%%%%%%%%%%%%%%%%%%%%%%%%%%%%%%%%%%%%%%%%%%%%%%%%%%%%
2   %
3   %  HC3N.m
4   %
5   %  Neutral Density Profile - HC3N
6   %  Yung and Toublanc models
7   %
8   %  Karin Agren, Swedish Institute of Space Physics, Uppsala, 2005.
9   %%%%%%%%%%%%%%%%%%%%%%%%%%%%%%%%%%%%%%%%%%%%%%%%%%%%%%%%%%%%%%%%%%%%%%%%%%%%%%%
10
11  % Values taken from the Yung and Toublanc models
12  % 1 = Yung, 2 = Toublanc
13
14  x_HC3N1 = [800 890 1010 1100 1210 1325 1460 1680]';
15  x_HC3N2 = [775 830 925 1015 1100 1195 1305 1425]';
16
17  N_HC3N1 = [4e7 1e7 1e6 1e5 1e4 1e3 1e2 1e1]';
18  N_HC3N2 = [4e7 1e7 1e6 1e5 1e4 1e3 1e2 1e1]';
19
20  % Finding the appropriate equations
21
22  x_HC3N1t = log (x_HC3N1);
23  N_HC3N1t = log (N_HC3N1);
24  x_HC3N2t = log (x_HC3N2);
25  N_HC3N2t = log (N_HC3N2);
26
27  A_HC3N1 = [x_HC3N1t.^0 x_HC3N1t.^1];
28  A_HC3N2 = [x_HC3N2t.^0 x_HC3N2t.^1];
29
30  a_HC3N1 = A_HC3N1\N_HC3N1t;
31  a_HC3N2 = A_HC3N2\N_HC3N2t;
32
33  % Plot
34
35  xm = linspace(700, 2700);
36  Nm_HC3N1 = exp(a_HC3N1(1))*xm.^a_HC3N1(2);
37  Nm_HC3N2 = exp(a_HC3N2(1))*xm.^a_HC3N2(2);
38
39  semilogx (Nm_HC3N1, xm, '-', Nm_HC3N2, xm, '--',N_HC3N1,x_HC3N1,'+',N_HC3N2,x_HC3N2,'*')
40
41  % Save data
42
43  save HC3N a_HC3N1 a_HC3N2
44
```

B.3.2 C2H4.m

```
1   %%%%%%%%%%%%%%%%%%%%%%%%%%%%%%%%%%%%%%%%%%%%%%%%%%%%%%%%%%%%%%%%%%%%%%%%%%%%%%%%
2   %
3   %  C2H4.m
4   %
5   %  Neutral Density Profile - C2H4
6   %  Yung and Toublanc models
7   %
8   %  Karin Agren, Swedish Institute of Space Physics, Uppsala, 2005.
9   %%%%%%%%%%%%%%%%%%%%%%%%%%%%%%%%%%%%%%%%%%%%%%%%%%%%%%%%%%%%%%%%%%%%%%%%%%%%%%%%
10
11  % Values taken from the Yung and Toublanc models
12  % 1 = Yung, 2 = Toublanc
13
14  x_C2H41 = [890 1110 1310 1525 1785 2075]';
15  x_C2H42 = [880 1075 1265 1465 1705 1985]';
16
17  N_C2H41 = [1e8 1e7 1e6 1e5 1e4 1e3]';
18  N_C2H42 = [1e8 1e7 1e6 1e5 1e4 1e3]';
19
20  % Finding the appropriate equations
21
22  x_C2H41t = log (x_C2H41);
23  N_C2H41t = log (N_C2H41);
24  x_C2H42t = log (x_C2H42);
25  N_C2H42t = log (N_C2H42);
26
27  A_C2H41 = [x_C2H41t.^0 x_C2H41t.^1];
28  A_C2H42 = [x_C2H42t.^0 x_C2H42t.^1];
29
30  a_C2H41 = A_C2H41\N_C2H41t;
31  a_C2H42 = A_C2H42\N_C2H42t;
32
33  % Plot
34
35  xm = linspace(700, 2700);
36  Nm_C2H41 = exp(a_C2H41(1))*xm.^a_C2H41(2);
37  Nm_C2H42 = exp(a_C2H42(1))*xm.^a_C2H42(2);
38
39  semilogx (Nm_C2H41, xm, '-', Nm_C2H42, xm, '--',N_C2H41,x_C2H41,'+',N_C2H42,x_C2H42,'*')
40
41  % Save data
42
43  save C2H4 a_C2H41 a_C2H42
44
```

B.3.3   HCNingo.m

```
1    %%%%%%%%%%%%%%%%%%%%%%%%%%%%%%%%%%%%%%%%%%%%%%%%%%%%%%%%%%%%%%%%%%%%%%%%%%%%%%%%%%%%
2    %
3    %  HCNingo.m
4    %
5    %  Neutral Density Profile - HCN
6    %  Ingo's model
7    %
8    %  Karin Agren, Swedish Institute of Space Physics, Uppsala, 2005.
9    %%%%%%%%%%%%%%%%%%%%%%%%%%%%%%%%%%%%%%%%%%%%%%%%%%%%%%%%%%%%%%%%%%%%%%%%%%%%%%%%%%%%
10
11   % Load data
12
13   load HCN
14
15   % Values achieved from Muller--Wodarg
16
17   x_HCNi = [621.502 642.983 664.523 686.215 708.134 730.340 752.854 775.658 ...
18       798.706 821.946 845.344 868.889 892.600 916.520 940.710 965.238 990.172 ...
19       1015.58 1041.51 1068.00 1095.10 1122.84 1151.23 1180.30 1210.10 1240.66 ...
20       1272.04 1304.30 1337.55 1371.89 1407.49 1444.54 1483.34 1524.28 1567.94 ...
21       1615.20 1667.43]';
22
23   N_HCNi = [3.68193e7 3.72162e7 3.71318e7 3.68136e7 3.63866e7 3.59387e7 ...
24       3.55124e7 3.50444e7 3.42701e7 3.27771e7 3.02814e7 2.68327e7 2.27731e7 ...
25       1.85546e7 1.45712e7 1.10790e7 8.19376e6 5.92243e6 4.20281e6 2.94015e6 ...
26       2.03438e6 1.39581e6 951370 644978 435260 292502 195752 130430 86480 ...
27       57011.4 37325.1 24228.2 15557.1 9849.93 6120.92 3707.31 2164.82]';
28
29   % Finding the appropriate equation
30
31   x_HCNit = log (x_HCNi);
32   N_HCNit = log (N_HCNi);
33
34   A_HCNi = [x_HCNit.^0 x_HCNit.^1];
35
36   a_HCNi = A_HCNi\N_HCNit;
37
38   % Plot
39
40   xm = linspace(600,1667,1067);
41   Nm_HCNi = exp(a_HCNi(1))*xm.^a_HCNi(2);
42
43   HCNin1 = interp1(x_HCNi, N_HCNi,xm);
44   pip = linspace(1668,2000,332)
45   HCNin2 = exp(a_HCN2(1)).*pip.^a_HCN2(2);
46
47   HCNin = [HCNin1 HCNin2]
48   mjau = [xm,pip]
49
50   semilogx (HCNin,mjau)
51   xlabel('Density [cm^{-3}]')
52   ylabel('Altitude [km]')
53
54   % Save data
55
56   save HCNi HCNin
57
58
```

B.4 Density profiles

B.4.1 ionz.m

```matlab
%%%%%%%%%%%%%%%%%%%%%%%%%%%%%%%%%%%%%%%%%%%%%%%%%%%%%%%%%%%%%%%%%%%%%%%%%%%%%%%%%%%%%
%
%  ionz.m
%
%  Script that produces a density profile for Titan for electrons of
%  various flux and energy (Flyby T5)
%
%  Karin Agren, Swedish Institute of Space Physics, Uppsala, 2006.
%%%%%%%%%%%%%%%%%%%%%%%%%%%%%%%%%%%%%%%%%%%%%%%%%%%%%%%%%%%%%%%%%%%%%%%%%%%%%%%%%%%%%

%%% Read data

load atm.mat
load dep.mat

%%% Input parameters

% altitude [km]
alt = linspace (800,2000,1200);

% electron flux [cm-2 s-1]
F = input('flux  = ');

% electron energy [eV]
E = input('electron energy [eV] = ');

% energy loss per ion pair formation [eV]
D = 37;

% effective range [g cm-2]
R = 4.30e-7+5.36e-6*(E/1000)^1.67;

% density [g cm-3]
ro = exp( a_N2(1) ) .* alt.^a_N2(2) .* (28*1.00798*1.66054e-27*1000);

% JWE
  ro_flip = fliplr( ro );
  s_flip  = cumsum( ro_flip ) .* 100000;
  s       = fliplr( s_flip );

% Energy deposition
  sR      = s ./ R;

  % Monodirectional beam
  Lambda_uni      = zeros( 1, length(alt) );
  tmp             = polyval( p_uni, sR );
  ind             = find( sR <= 1 );
  Lambda_uni(ind) = tmp(ind);

  % Isodirectional beam
  Lambda_iso      = zeros( 1, length(alt) );
  tmp             = polyval( p_iso, sR );
  ind             = find( sR <= 1 );
  Lambda_iso(ind) = tmp(ind);

%%% Computation of the ionisation rate
  q_uni = (F*E) .* Lambda_uni .* ro ./(R*D);
  q_iso = (F*E) .* Lambda_iso .* ro ./(R*D);

%%% Plot

  %semilogx( q_uni , alt, 'r')
```

```
63     %hold on;
64     %   semilogx( q_iso , alt, 'b')
65     %hold off;
66     %legend ('Unidirectional', 'Isotropic')
67     %grid;
68     %xlabel('Ionisation rate [cm^{-3} s^{-1}]')
69     %ylabel('Altitude [km]')
70
71     %%% Save data
72
73        save q q_uni q_iso alt E
74
75     %%%%%%%%%%%%%%%%%%%%%%%%%%%%%%%%%%%%%%%%%%%%%%%%%%%%%%%%%%%%%%%%%%%%%%%%%%%
76     %%%%%% Former electron m.file
77     %%%%%%%%%%%%%%%%%%%%%%%%%%%%%%%%%%%%%%%%%%%%%%%%%%%%%%%%%%%%%%%%%%%%%%%%%%%
78
79     %%% Read data
80
81     load q.mat
82     load atm.mat
83     load HCNi.mat
84     load HC3N.mat
85     load C2H4.mat
86
87     nCH4 = exp(a_CH4(1))*alt.^a_CH4(2);
88     nHCNi = interp1(mjau,HCNin,alt);
89     nHC3N1 = exp(a_HC3N1(1))*alt.^a_HC3N1(2);
90     nHC3N2 = exp(a_HC3N2(1))*alt.^a_HC3N2(2);
91     nC2H41 = exp(a_C2H41(1))*alt.^a_C2H41(2);
92     nC2H42 = exp(a_C2H42(1))*alt.^a_C2H42(2);
93
94     %%% Constants
95
96     k2 = 9.12e-10; % [cm3 s-1]
97     k3 = 1.1e-9; % [cm3 s-1]
98     k4 = 2.7e-9; % [cm3 s-1]
99     k5 = 3.4e-9; % [cm3 s-1]
100    k6 = 3.55e-9; % [cm3 s-1]
101    k7 = 1.3e-9; % [cm3 s-1]
102    Te = 700; % [K]
103    alfa = 6.4e-7*sqrt(300/Te); % [cm3 s-1]
104
105    %%% Choose angular dispersion
106
107    d = input('Unidirectional = 1, Isotropic = 2 : ');
108
109    if d == 1
110
111    %%% Unidirectional
112
113    %%% Yung's model [1]
114
115    nN2plus1 = q_uni ./ (k2.*nCH4);
116
117    nCH3plus1 = k2.*nN2plus1/k3;
118
119    nC2H5plus1 = k3.*nCH3plus1.*nCH4./(k4.*nHCNi);
120
121    nH2CNplus1 = - nC2H5plus1/2 + sqrt((nC2H5plus1/2).^2+k4.*nC2H5plus1 .* ...
122        nHCNi/alfa);
123
124    nC3H2Nplus1 = (k5 .* nH2CNplus1 .* nHC3N1 + k6 .* nC2H5plus1 .* nHC3N1) ...
125        ./ (k7 .* nC2H41);
126
127    groda = (nC2H5plus1 + nH2CNplus1 + nC3H2Nplus1) ./ 2;
128
129    nC5H5Nplus1 = - groda + sqrt((groda).^2 + k7 .* nC3H2Nplus1 .* nC2H41 ...
130        ./ alfa);
131
132    yne = nN2plus1 + nCH3plus1 +  nC2H5plus1 + nH2CNplus1 + nC3H2Nplus1 + ...
133        nC5H5Nplus1;
134
135    %%% Toublanc's model [2]
136
137    nN2plus2 = q_uni ./ (k2.*nCH4);
138
139    nCH3plus2 = k2.*nN2plus2/k3;
```

```
140
141     nC2H5plus2 = k3.*nCH3plus2.*nCH4./(k4.*nHCNi);
142
143     nH2CNplus2 = - nC2H5plus2/2 + sqrt((nC2H5plus2/2).^2+k4.*nC2H5plus2 .* ...
144         nHCNi/alfa);
145
146     nC3H2Nplus2 = (k5 .* nH2CNplus2 .* nHC3N2 + k6 .* nC2H5plus2 .* nHC3N2) ...
147         ./ (k7 .* nC2H42);
148
149     padda = (nC2H5plus2 + nH2CNplus2 + nC3H2Nplus2) ./ 2;
150
151     nC5H5Nplus2 = - padda + sqrt((padda).^2 + k7 .* nC3H2Nplus2 .* nC2H42 ...
152         ./ alfa);
153
154     tne = nN2plus2 + nCH3plus2 + nC2H5plus2 + nH2CNplus2 + nC3H2Nplus2 + ...
155         nC5H5Nplus2;
156
157     % version 1 - electrons
158     %subplot(2,1,2)
159     %semilogx(tne, alt,'r')
160     %legend ('','Toublanc e^-')
161
162     % version 2 - all
163     %semilogx(nN2plus2, alt, '-.', nCH3plus2, alt, '-.', nC2H5plus2, alt, ...
164     '--', nH2CNplus2, alt, '--', nC3H2Nplus2, alt, '--', nC5H5Nplus2, alt, ...
165     '--', tne, alt, '--', nC2H5plus1, alt, nH2CNplus1, alt, nC3H2Nplus1, ...
166     alt, nC5H5Nplus1, alt, yne, alt)
167     %legend ('N_2+', 'CH_3+', 'Toublanc C_2H_5+', 'Toublanc H_2CN+', ...
168     'Toublanc C_3H_2N+', 'Toublanc C_5H_5N+', 'Toublanc e^-', ...
169     'Yung C_2H_5+', 'Yung H_2CN+', 'Yung C_3H_2N+', 'Yung C_5H_5N+', ...
170     'Yung e^-')
171
172     % version 3 - ions
173     semilogx(nC2H5plus2, alt, '--', nH2CNplus2, alt, '--', nC3H2Nplus2, ...
174         alt, '--', nC5H5Nplus2, alt, '--', tne, alt, '--', nC2H5plus1, ...
175         alt, nH2CNplus1, alt, nC3H2Nplus1, alt, nC5H5Nplus1, alt, yne, alt)
176     legend ('Toublanc C_2H_5+', 'Toublanc H_2CN+','Toublanc C_3H_2N+', ...
177         'Toublanc C_5H_5N+', 'Toublanc e^-', 'Yung C_2H_5+', 'Yung H_2CN+', ...
178         'Yung C_3H_2N+', 'Yung C_5H_5N+', 'Yung e^-')
179
180     xlabel('Density [cm^{-3}]')
181     ylabel('Altitude [km]')
182     title (['Unidirectional (', num2str(E),' eV)'])
183
184     else
185
186     %%% Isotropic
187
188     %%% Yung's model [1]
189
190     nN2plus1 = q_iso ./ (k2.*nCH4);
191
192     nCH3plus1 = k2.*nN2plus1/k3;
193
194     nC2H5plus1 = k3.*nCH3plus1.*nCH4./(k4.*nHCNi);
195
196     nH2CNplus1 = - nC2H5plus1/2 + sqrt((nC2H5plus1/2).^2+k4.*nC2H5plus1 .* ...
197         nHCNi/alfa);
198
199     nC3H2Nplus1 = (k5 .* nH2CNplus1 .* nHC3N1 + k6 .* nC2H5plus1 .* nHC3N1) ...
200         ./ (k7 .* nC2H41);
201
202     groda = (nC2H5plus1 + nH2CNplus1 + nC3H2Nplus1) ./ 2;
203
204     nC5H5Nplus1 = - groda + sqrt((groda).^2 + k7 .* nC3H2Nplus1 .* nC2H41 ...
205         ./ alfa);
206
207     yne = nN2plus1 + nCH3plus1 +  nC2H5plus1 + nH2CNplus1 + nC3H2Nplus1 + ...
208         nC5H5Nplus1;
209
210     %%% Toublanc's model [2]
211
212     nN2plus2 = q_iso ./ (k2.*nCH4);
213
214     nCH3plus2 = k2.*nN2plus2/k3;
215
216     nC2H5plus2 = k3.*nCH3plus2.*nCH4./(k4.*nHCNi);
```

```
217
218    nH2CNplus2 = - nC2H5plus2/2 + sqrt((nC2H5plus2/2).^2+k4.*nC2H5plus2.* ...
219        nHCNi/alfa);
220
221    nC3H2Nplus2 = (k5 .* nH2CNplus2 .* nHC3N2 + k6 .* nC2H5plus2 .* nHC3N2) ...
222        ./ (k7 .* nC2H42);
223
224    padda = (nC2H5plus2 + nH2CNplus2 + nC3H2Nplus2) ./ 2;
225
226    nC5H5Nplus2 = - padda + sqrt((padda).^2 + k7 .* nC3H2Nplus2 .* nC2H42 ...
227        ./ alfa);
228
229    tne = nN2plus2 + nCH3plus2 + nC2H5plus2 + nH2CNplus2 + nC3H2Nplus2 + ...
230        nC5H5Nplus2;
231
232    % version 1 - electrons
233    %semilogx( tne, alt, 'c-', yne, alt, 'b--')
234    %legend('Toublanc e^-','Yung e^-')
235
236    % version 2 - all
237    %semilogx(nN2plus2, alt, '-.', nCH3plus2, alt, '-.', nC2H5plus2, alt, ...
238    '--', nH2CNplus2, alt, '--', nC3H2Nplus2, alt, '--', nC5H5Nplus2, alt, ...
239        '--', tne, alt, '--', nC2H5plus1, alt, nH2CNplus1, alt, ...
240        nC3H2Nplus1, alt, nC5H5Nplus1, alt, yne, alt)
241    %legend ('N_2+', 'CH_3+', 'Toublanc C_2H_5+', 'Toublanc H_2CN+', ...
242    'Toublanc C_3H_2N+', 'Toublanc C_5H_5N+', 'Toublanc e^-', ...
243        'Yung C_2H_5+', 'Yung H_2CN+', 'Yung C_3H_2N+', 'Yung C_5H_5N+', ...
244        'Yung e^-')
245
246    % version 3 - ions
247    semilogx(nC2H5plus2, alt, '--', nH2CNplus2, alt, '--', nC3H2Nplus2, ...
248        alt, '--', nC5H5Nplus2, alt, '--', tne, alt, '--', nC2H5plus1, alt, ...
249        nH2CNplus1, alt, nC3H2Nplus1, alt, nC5H5Nplus1, alt, yne, alt)
250    legend ('Toublanc C_2H_5+', 'Toublanc H_2CN+','Toublanc C_3H_2N+', ...
251        'Toublanc C_5H_5N+', 'Toublanc e^-', 'Yung C_2H_5+', 'Yung H_2CN+', ...
252        'Yung C_3H_2N+', 'Yung C_5H_5N+', 'Yung e^-')
253
254    xlabel('Density [cm^{-3}]')
255    ylabel('Altitude [km]')
256    title (['Isotropic (', num2str(E),' eV)'])
257
258    end
259
260    %%% Finding maxima
261
262    maxelectron = max(tne)
263    y = find (tne==max(tne));
264    maxalt = alt(y)
265
266    %%% Plot
267
268    semilogx(tne,alt,'r')
```

B.4.2 density.m

```matlab
%%%%%%%%%%%%%%%%%%%%%%%%%%%%%%%%%%%%%%%%%%%%%%%%%%%%%%%%%%%%%%%%%%%%%%%%%%%%%%%%
%
%  density.m
%
%  The electron density measured by the Langmuir probe onboard Cassini
%
%  Karin Agren, Swedish Institute of Space Physics, Uppsala, 2005.
%%%%%%%%%%%%%%%%%%%%%%%%%%%%%%%%%%%%%%%%%%%%%%%%%%%%%%%%%%%%%%%%%%%%%%%%%%%%%%%%

%%% Load data

load LP_T5_altNe20.dat

%%% Processing data

LP_T5_altNe20;
alt1 = LP_T5_altNe20(:,7);
RT = 2575; % km
alti = alt1 * RT - RT;
dens = LP_T5_altNe20(:,8);

%%% Removal of NaN

A = [alti, dens];
n1 = isnan(A);
B = n1(:,2);
o = find (B==1);
A(o,:) = [];

%%% Dividing into vectors

alti = A(:,1);
dens = A(:,2);

%%% Removal of high altitude values

p = find (alti>=1700);
alti(p) = [];
dens(p) = [];

%%% Removal of the inbound track

q = find (alti == min(alti));
alti(1:max(q) - 1 ) = [];
dens(1:max(q) - 1) = [];

%%% Plot

semilogx(dens, alti,'k')
xlabel('Density [cm^{-3}]')
ylabel('Altitude [km]')
```

B.5   Additional modelling

These scripts are shown for $E = 150$ eV, but are also applicable for other values.

B.5.1   nitrogen150.m

```matlab
%%%%%%%%%%%%%%%%%%%%%%%%%%%%%%%%%%%%%%%%%%%%%%%%%%%%%%%%%%%%%%%%%%%%%%%%%%%%
%
%  nitrogen150.m
%
%  Ionisation rates for electron energies lower than 200 eV
%  Based on the model by Prof. Lummerzheim
%
%  Karin Agren, Swedish Institute of Space Physics, Uppsala, 2006.
%%%%%%%%%%%%%%%%%%%%%%%%%%%%%%%%%%%%%%%%%%%%%%%%%%%%%%%%%%%%%%%%%%%%%%%%%%%%

% Load data

load atm

%  Calculations of column density

E = 150; % eV

xm = linspace(800, 2000, 1200);
Nm_N2 = exp(a_N2(1))*xm.^a_N2(2);

  N2_flip = fliplr( Nm_N2 );
  s_flip  = cumsum( N2_flip ) .* 100000 ;
  dens150      = fliplr( s_flip );

% Reading in data

fp = fopen('titan_150.txt','r');
x = fgetl(fp);
x = fgetl(fp);

for i = 1:201

x = str2num(fgetl(fp));
n(i) = x(3);
io(i) = x(4);
i = i + 1;
end

% Interpolation between the two

new150 = interp1 (n, io, dens150);

% Plot

semilogx(new150, xm)
xlabel('Ionisation rate [cm^{-3} s^{-1}]')
ylabel('Altitude [km]')
title ([ num2str(E),' eV'])

% Finding maxima

peak1 = find(new150>=max(new150))
sprintf('Ionisation maximum at %d km', peak1)
peak2 = max(new150);
sprintf('Ionisation maximum at %d cm^{-3}', peak2)

% Save data

save dirk150 new150
```

B.5.2 dirkdens150.m

```
1   %%%%%%%%%%%%%%%%%%%%%%%%%%%%%%%%%%%%%%%%%%%%%%%%%%%%%%%%%%%%%%%%%%%%%%%%%%%%%%%%%%%%
2   %
3   %  dirkdens150.m
4   %
5   %  Using Prof. Lummerzheim's q to create a density profile
6   %
7   %  Karin Agren, Swedish Institute of Space Physics, Uppsala, 2006.
8   %%%%%%%%%%%%%%%%%%%%%%%%%%%%%%%%%%%%%%%%%%%%%%%%%%%%%%%%%%%%%%%%%%%%%%%%%%%%%%%%%%%%
9
10  %%% Read data
11
12  load dirk150.mat
13  load atm.mat
14  load HCN.mat
15  load HC3N.mat
16  load C2H4.mat
17
18  xm150 = xm;
19
20  nCH4 = exp(a_CH4(1))*xm150.^a_CH4(2);
21  nHCN1 = exp(a_HCNi(1))*xm150.^a_HCNi(2);
22  nHCN2 = exp(a_HCNi(1))*xm150.^a_HCNi(2);
23  nHC3N1 = exp(a_HC3N1(1))*xm150.^a_HC3N1(2);
24  nHC3N2 = exp(a_HC3N2(1))*xm150.^a_HC3N2(2);
25  nC2H41 = exp(a_C2H41(1))*xm150.^a_C2H41(2);
26  nC2H42 = exp(a_C2H42(1))*xm150.^a_C2H42(2);
27
28  %%% Constants
29
30  k2 = 9.12e-10; % [cm3 s-1]
31  k3 = 1.1e-9; % [cm3 s-1]
32  k4 = 2.7e-9; % [cm3 s-1]
33  k5 = 3.4e-9; % [cm3 s-1]
34  k6 = 3.55e-9; % [cm3 s-1]
35  k7 = 1.3e-9; % [cm3 s-1]
36  Te = 700; % [K]
37  alfa = 6.4e-7*sqrt(300/Te); % [cm3 s-1]
38
39  %%% Unidirectional
40
41  %%% Toublanc's model [2]
42
43  nN2plus2 = 3e-1 * 1.5e-4 * new150 ./ (k2.*nCH4);
44
45  nCH3plus2 = k2.*nN2plus2/k3;
46
47  nC2H5plus2 = k3.*nCH3plus2.*nCH4./(k4.*nHCNi);
48
49  nH2CNplus2 = - nC2H5plus2/2 + sqrt((nC2H5plus2/2).^2+k4.*nC2H5plus2.*nHCNi/alfa);
50
51  nC3H2Nplus2 = (k5 .* nH2CNplus2 .* nHC3N2 + k6 .* nC2H5plus2 .* nHC3N2) ./ (k7 .* nC2H42);
52
53  padda = (nC2H5plus2 + nH2CNplus2 + nC3H2Nplus2) ./ 2;
54
55  nC5H5Nplus2 = - padda + sqrt((padda).^2 + k7 .* nC3H2Nplus2 .* nC2H42 ./ alfa);
56
57  tne150 = nN2plus2 + nCH3plus2 + nC2H5plus2 + nH2CNplus2 + nC3H2Nplus2 + nC5H5Nplus2;
58
59  %%% Finding maxima
60
61  z = max(tne150);
62  f = find(tne150==max(tne150));
63  mu = xm150(f);
64  sprintf('Density maximum at %d km', mu)
65  sprintf('Density maximum at %d cm^{-3}', z)
66
```

```
67    %%% Plot
68
69    semilogx(tne150, xm150)
70    xlabel('Density [cm^{-3}]')
71    ylabel('Altitude [km]')
72
73    %%% Save data
74
75    save ionz150 tne150 xm150
76
```

BIBLIOGRAPHY

[1] A. F. Nagy and T. E. Cravens. Titans ionosphere : a review. *Planetary and Space Science*, 46:1149–1155, October 1998.

[2] J.-E. Wahlund, R. Boström, G. Gustafsson, D. A. Gurnett, W. S. Kurth, A. Pedersen, T. F. Averkamp, G. B. Hospodarsky, A. M. Persoon, P. Canu, F. M. Neubauer, M. K. Dougherty, A. I. Eriksson, M. W. Morooka, R. Gill, M. André, L. Eliasson, and I. Müller-Wodarg. Cassini Measurements of Cold Plasma in the Ionosphere of Titan. *Science*, 308:986–989, May 2005.

[3] D. A. Gurnett, W. S. Kurth, D. L. Kirchner, G. B. Hospodarsky, T. F. Averkamp, P. Zarka, A. Lecacheux, R. Manning, A. Roux, P. Canu, N. Cornilleau-Wehrlin, P. Galopeau, A. Meyer, R. Boström, G. Gustafsson, J.-E. Wahlund, L. Åhlen, H. O. Rucker, H. P. Ladreiter, W. Macher, L. J. C. Woolliscroft, H. Alleyne, M. L. Kaiser, M. D. Desch, W. M. Farrell, C. C. Harvey, P. Louarn, P. J. Kellogg, K. Goetz, and A. Pedersen. The Cassini Radio and Plasma Wave Investigation. *Space Science Reviews*, 114:395–463, September 2004.

[4] S. H. Høymork and I Sandahl. *Sensors and Instruments for Space Exploration*. Swedish Institute of Space Physics, Kiruna, 2002.

[5] R. V. Yelle. Presentation at Titan Workshop, Crete, 2005.

[6] D. Toublanc, J. P. Parisot, J. Brillet, D. Gautier, F. Raulin, and C. P. McKay. Photochemical modeling of Titan's atmosphere. *Icarus*, 113:2–26, January 1995.

[7] Y. L. Yung, M. Allen, and J. P. Pinto. Photochemistry of the atmosphere of Titan - Comparison between model and observations. *Astrophysical Journal Supplement Series*, 55:465–506, July 1984.

[8] Y. L. Yung. An update of nitrile photochemistry on Titan. *Icarus*, 72:468–472, November 1987.

[9] R. V. Yelle. Non-LTE models of Titan's upper atmosphere. *Astrophysical Journal*, 383:380–400, December 1991.

[10] I. Müller Wodarg. Private communication, 2006.

[11] M. H. Rees. *Physics and chemistry of the upper atmosphere.* Cambridge University Press, Cambridge, 1989.

[12] M. H. Rees. Auroral ionization and excitation by incident energetic electrons. *Planetary and Space Science*, 11:1209–+, October 1963.

[13] D. Lummerzheim. Private communication, 2005.

[14] C. N. Keller, V. G. Anicich, and T. E. Cravens. Model of Titans ionosphere with detailed hydrocarbon ion chemistry. *Planetary and Space Science*, 46:1157–1174, October 1998.

[15] T. E. Cravens, I. P. Robertson, J. Clark, J.-E. Wahlund, J. H. Waite, S. A. Ledvina, H. B. Niemann, R. V. Yelle, W. T. Kasprzak, J. G. Luhmann, R. L. McNutt, W.-H. Ip, V. De La Haye, I. Müller-Wodarg, D. T. Young, and A. J. Coates. Titan's ionosphere: Model comparisons with Cassini Ta data. *Geophysical Research Letters*, 32:12108–+, June 2005.

[16] T. E. Cravens et al. *Geophysical Research Letters*, 2006. Accepted.